6.2 PRODUCING GRIDDED PROBABILISTIC GUIDANCE FOR WARM SEASON LIGHTNING OVER FLORIDA

Phillip E. Shafer and Henry E. Fuelberg *
Department of Meteorology
Florida State University
Tallahassee, FL

1. INTRODUCTION

Improved forecasts of cloud-to-ground (CG) lightning would yield many societal benefits. Skillful probabilistic guidance in the 3-12 h time frame would allow the public to better assess the CG lightning threat and thereby support better decision-making regarding the protection of life and property. Some of the economic sectors that would benefit include organizers of outdoor sporting events, the fire weather community, aviation, the maritime industry, outdoor construction, and electric utilities. A technique that produces accurate and timely CG lightning threat information should lead to reduced fatalities and injuries.

Florida annually receives more CG strikes than any other state (Orville 1994; Hodanish et al. 1997; Orville and Huffines 2001; and Orville et al. 2002). Warm season convection over Florida is regulated by low-level convergence associated with the sea breeze. Interactions between the sea breeze, the prevailing wind, coastline curvature, and even urban effects have been shown to influence lightning patterns (e.g., López and Holle 1987; Arritt 1993; Lericos et al. 2002; Westcott 1995; Steiger et al. 2002). Even if one could forecast the exact locations that will experience deep convection, it does not necessarily follow that these areas will experience the most lightning, since lightning production ultimately is controlled by cloud microphysics. Thorough descriptions of cloud electrification processes are given in Reynolds et al. (1957), Vonnegut (1963), Williams (1985), Williams et al. (1989), Price and Rind (1992) and Petersen and Rutledge (1998).

A variety of statistical techniques have been used to develop forecast models for thunderstorms and lightning, including multiple linear regression (MLR) for continuous predictands (e.g., Neumann and Nicholson 1972; Reap and MacGorman 1989), or binary logistic regression (BLR) for binary "yes" or "no" predictands (e.g., Livingston et al. 1996; Mazany et al. 2002; Lambert et al. 2005; and Shafer and Fuelberg 2006). Statistical prediction models for lightning over Canada and the northern U.S. also have been developed using Classification and Regression Trees (CART) (Burrows et al. 2005).

Many studies have utilized parameters derived from morning soundings to forecast afternoon lightning. However, this approach sometimes can produce large forecast errors if morning conditions change, or if the sounding is not representative of the entire forecast area. An alternative approach is to use data from numerical weather prediction (NWP) models. A method known as Model Output Statistics (MOS; Glahn and Lowry 1972) often has been used to relate forecast output from NWP models to a predictand of interest. However, MOS has several drawbacks that can limit its forecast skill. Since NWP models are constantly changing, it often is difficult to obtain a sufficiently long archive of forecasts from the same model to develop the MOS equations. Any modifications to the NWP model that change (even reduce) systematic model errors require redevelopment of the MOS equations (Wilks 2006).

An alternative to MOS is the perfect prognosis (PP) (or "perfect prog") method. This approach develops statistical relationships between observed atmospheric parameters and observations of the predictand (Klein et al. 1959; Klein 1971). Bothwell (2002) used the PP method to develop lightning guidance for the western U.S. on a 40 × 40 km grid, using analyses from the NCEP 40-km RUC (RUC40).

A drawback to the PP scheme is that it assumes a "perfect" forecast of the predictors by the NWP model and thus does not account for model biases. Conversely, a significant advantage is the stability of the equations. Since PP equations are developed without NWP information, any changes to the driving NWP models do not require redevelopment of the PP equations. In fact, improved

*Corresponding author address:
Henry E. Fuelberg, Dept. of Meteorology, Florida State University, Tallahassee, FL 32306-4520; e-mail:fuelberg@met.fsu.edu

random or systematic errors in the NWP model should improve the statistical forecasts (Wilks 2006). This advantage makes PP the method of choice for this study.

We use the PP method to develop a high-resolution, gridded forecast guidance product for warm season CG lightning over Florida on a 10 × 10 km grid at 3-hourly intervals. An archive of analyses from the 20-km RUC model (RUC20) is used to examine relationships between observed atmospheric parameters and spatial and temporal patterns of CG lightning. The most important RUC-derived parameters then are used to develop equations producing 3-hourly forecasts of the probability of one or more CG flashes (PROB≥1), as well as the probability of exceeding various flash count percentile thresholds (PROB≥T). Finally, the equations are applied to output from three mesoscale models during an independent test period (the 2006 warm season).

Section 2 describes the study domain as well as the lightning and RUC analysis datasets. The model development procedure is described in Section 3. A discussion of the parameters comprising the models and their physical significance to lightning occurrence is given in Section 4. Section 5 evaluates the utility of the lightning forecast scheme when applied to output from several mesoscale models during the 2006 warm season. Finally, a summary of the model development and verification results is given in Section 6.

2. DATA

Our lightning guidance was developed for all of Florida (Fig. 1), covering the Peninsula and Panhandle and extending northward into southeast Alabama and southern Georgia. Figure 1 also shows the 10 × 10-km grid points used for computing the lightning probabilities.

We utilized CG lightning data from the National Lightning Detection Network (NLDN) (Cummins et al. 1998). A detailed description of its sensors and methods of detection is given in Cummins et al. (1998). We employed a quality control procedure recommended by Cummins et al. (1998) to remove possible cloud discharges and duplicate strikes. This procedure is described in detail in Shafer and Fuelberg (2006).

At every grid point over land (Fig. 1), flash totals were tabulated for each 3-h period (e.g., 0000-0259 UTC, …, 2100-2359 UTC) by summing the strikes that occurred within a 10 km radius. The flash totals then were transformed into binary variables; "1" if one or more flashes occurred during the 3-h period or "0" if no lightning occurred. Additional binary variables were assigned based on whether the flash total exceeded the 50^{th}, 75^{th}, 90^{th}, or 95^{th} percentiles during a given 3-h period (values are given in Table 1 for the four most active 3-h periods). The 3-h flash totals and binary indicators served as the predictands for developing the lightning forecast equations.

Observed atmospheric predictors were obtained from an archive of RUC analyses during the 2002-2005 warm seasons (~ 600 days). A complete description of the RUC model is given in Benjamin et al. (2002, 2004). The atmospheric parameters calculated from the RUC analyses are described in Section 3.

We used S-PLUS version 6.1 for Windows and the Statistical Package for the Social Sciences (SPSS) version 11.5 for Windows for the exploratory analyses and statistical modeling. Both are powerful, state-of-the-art packages with a wide range of analysis and modeling capabilities.

3. MODEL DEVELOPMENT

3.1 *Climatological and Map Type Predictors*

Climatological and pattern type lightning frequencies were developed as candidate predictors to capture local enhancements due to interactions between the low-level wind, thermal circulations, and coastline topography (e.g., Pielke 1974; Arritt 1993; Laird et al. 1995; Lericos et al. 2002). These predictors have the potential to add detailed information about local effects that may not be well resolved by NWP models (Reap 1994a).

We used a simple correlation technique described in Lund (1963) and Reap (1994a) to develop the map type predictors. Based on Reap (1994a), the correlation technique was applied to 3-hourly observed sea level pressure (SLP) fields from RUC analyses spanning the 1998-2005 warm seasons (~ 1224 days). SLP patterns imply both the direction and speed of the low-level flow. The pattern classification was performed over the geographical area shown in Fig. 1. To capture regional scale patterns (i.e., the prevailing wind) and to smooth small scale variations, the RUC SLP values were interpolated to a coarser grid (100 km) (Fig. 1), and the correlation technique was applied to the interpolated SLP values.

Table 2 shows results of the map type classification. Five map types (A-E) were developed using the Reap (1994a) technique. Types A and B comprise ~ 44% of the total sample, while types C-E comprise ~ 34%. The remaining ~ 22% of the sample could not be classified at the correlation threshold being used (0.70).

Using the binary indicators for one or more flashes (Section 2), relative lightning frequencies (MTFREQ) were calculated for each map type and 3-h period. Similarly, 3-h flash totals were used to calculate an unconditional mean number of flashes for each map type (MTMEAN). Climatological relative frequencies and unconditional means also were calculated using all warm season days during 1995-2005. The climatological and map type lightning frequencies and means were submitted as candidate predictors for the regression analysis described in Section 3.4.

Composite SLP patterns associated with each map type are shown in the left panels of Fig. 2, while the right panels show spatial distributions of the mean number of flashes (MTMEAN) for the 1800-2059 UTC period. The five map types represent distinctly different flow patterns, and are similar to those from previous studies (e.g., Reap 1994a; Lericos et al. 2002). The predominant pattern, type A (Figs. 2a-b), is characterized by high pressure northeast of Florida that produces prevailing easterly and southeasterly flow across the state. As a result, most of the lightning is confined to the West Coast, with maxima near Tampa Bay, Fort Myers, and east of Lake Okeechobee. Map type B (Figs. 2c-d) contains a surface ridge over South Florida that results in southwesterly flow across the state. This focuses the lightning along the East Coast of the Peninsula, with coastline interactions evident near the Big Bend of the Panhandle (Camp et al. 1998). Map type C (Figs. 2e-f) represents a transition between types A and B, in which the east-west oriented surface ridge is located over central Florida. This pattern produces southeasterly flow over South Florida and south-southwesterly flow over the northern Peninsula. Thus, the lightning patterns are a combination of types A and B, with maxima along both coasts. Map type D (Figs. 2g-h) is characterized by high pressure north of Florida and lower pressure to the southeast, which is most common during May and September after a cold frontal passage. The dry northeasterly flow confines most of the lightning to South Florida. Finally, map type E (Figs. 2i-j) is a variation of type B, exhibiting a lobe of high pressure over the Gulf of Mexico and lower pressure to the northeast. West-northwesterly flow confines most lightning to the East Coast and Big Bend, with generally less coverage than observed with type B.

3.2 *Model-Analyzed Candidate Predictors*

A large number of RUC-analyzed predictors were investigated for possible inclusion in the candidate predictor pool, many of which have been found useful in previous studies. The parameters investigated, their abbreviations, and a short description of each are listed in Table 3. The parameters were calculated from the RUC-analyzed temperature, dew point, wind, height, and surface pressure fields valid every 3 h (e.g., 0000 UTC, 0300 UTC,…, etc.). The fields were interpolated to the 10 × 10-km grid (Fig. 1) and transformed into the format of a vertical sounding at each grid point (Bothwell 2002).

3.3 *Generalized Linear Models*

MLR has been used in the majority of previous statistical lightning studies (e.g., Neumann and Nicholson 1972; Reap and Foster 1979; Reap and MacGorman 1989; Reap 1994a; Hughes 2001). However, unless the assumptions of constant variance and Gaussian residuals are met (which is rarely the case with count data), these methods can lead to undesirable and sometimes nonsensical results. Thus, we considered alternative regression methods; namely, the family of generalized linear models (GLMs).

When the predictand is either “yes” or “no”, one such method is binary logistic regression (BLR). A thorough description of BLR is given in Lehmiller et al. (1997) and Wilks (2006). We used BLR to develop equations giving the probability of one or more flashes (PROB≥1) within a 10-km radius of each grid point (Fig. 1) to produce spatial probability forecasts for each 3-h period. BLR has been used successfully in previous lightning forecasting studies (e.g., Bothwell 2002; Mazany et al. 2002; Lambert et al. 2005; Shafer and Fuelberg 2006).

Our second objective was to develop equations to forecast the amount of lightning during each 3-h period, conditional on one or more flashes occurring. The most appropriate model for count data is the Poisson family of GLMs (Elsner and Schmertmann 1993; Gardner et al. 1995; Elsner and Jagger 2004). As in BLR, this approach

employs a log link function to linearize the expected value (μ) of the dependent variable (y):

$$\ln(\mu[x_i]) = b_0 + b_1 x_1 + ... + b_K x_K \quad (1)$$

$$\mu[x_i] = \exp(b_0 + b_1 x_1 + ... + b_K x_K), \quad (2)$$

where $\mu[x_i]$ is the mean response resulting from the i^{th} set of predictors (x_1, x_2, …., x_K). If one assumes that events occur randomly and at a constant average rate (μ) with Var(y) = μ, then the events are said to be generated by a Poisson process with the probability model

$$\Pr(y \mid \mu) = \frac{\exp(-\mu)\mu^y}{y!}. \quad (3)$$

A histogram of the conditional count distribution for our most active lightning period (1800-2059 UTC) is shown in Fig. 3. It is clear that the counts are strongly skewed, with the majority of cases having 10 or less flashes and few cases having 100 or more flashes. Since the variance of the distribution is very large, ~ 80 times greater than the mean (μ ~23 flashes), the data do not fit the Poisson assumption that Var(y) = μ. The most likely explanation is that the counts were generated by an inhomogeneous Poisson process (also known as a Cox process), whereby the number of storms over a given region and the number of flashes produced per storm are both approximately Poisson. This "mixed" Poisson process results in the lightning counts having more dispersion than is accounted for by a homogeneous Poisson model (personal communication with Dr. Thomas Jagger, Department of Geography, FSU).

An alternative probability model is the negative binomial (NB) scheme. As in Poisson regression, the mean response (μ) is modeled by (2); however, the variance now is a quadratic function of μ :

$$\mathrm{Var}(y_i \mid \mu[x_i]) = \mu[x_i] + \theta^{-1}\mu[x_i]^2, \quad (4)$$

where θ^{-1} is the shape parameter (estimated by maximum likelihood). The resulting probability model for the number of flashes, y, as a function of μ and θ is given by:

$$\Pr(y \mid \mu[x_i], \theta) = \frac{\Gamma(y+\theta)}{y!\Gamma(\theta)}\left(\frac{\theta}{\theta+\mu[x_i]}\right)^{\theta}\left(\frac{\mu[x_i]}{\theta+\mu[x_i]}\right)^{y}, \quad (5)$$

where Γ is the gamma function (Crawley 2002).

Figure 4 shows the probability distributions implied by the Poisson (3) and NB (5) models with only the intercept term (b_0) included for μ = 23.15 and θ = 0.342 (estimated from the observed data using the S-PLUS software). Also shown is the observed frequency distribution. It is clear that the Poisson model is a poor choice for representing the count distribution since too little probability is assigned to the smallest lightning counts while too much is assigned to counts near the mean. The NB model is a much better fit to the data, capturing the large number of cases with 10 or fewer flashes and more closely representing the tail of the observed distribution.

Since the NB provides a much better fit to the observed frequency distribution (Fig. 4), it was our method of choice. The NB has been used previously to model thunderstorm activity at the Kennedy Space Center (KSC) (e.g., Falls et al. 1971, Williford et al. 1974) as well as thunderstorm and hail day probabilities in Nevada (Sakamoto 1973). However, to the best of our knowledge no prior study has used the NB as the probability model for lightning counts. Since the count distribution (Fig. 4) is left-truncated at one flash, the distribution is not strictly NB since (5) includes y = 0. However, if we treat y-1 as having a NB distribution, then (5) can be used to estimate the probability for each y-1. Since (5) is a probability density function, the individual probabilities (y = 1,∞) must sum to 1. Thus, the probability of meeting or exceeding any count threshold, T, can be obtained from

$$\Pr(y \geq T) = \sum_{y=T}^{\infty}\Pr(y) = 1 - \left(\sum_{y=1}^{T-1}\Pr(y)\right). \quad (6)$$

3.4. *Equation Development*

We determined whether relationships between observed predictors and lightning were generally the same for the entire study area or if they varied significantly from one portion of the state to another. We first subdivided the domain into nine areas (Fig. 5). Then, separate sets of equations were developed for each area (i.e., a regionalized operator approach), with the results compared to those obtained using a model developed for all

grid points (i.e., a generalized operator approach). A comparison of verification scores revealed that it would be sufficient to consolidate the nine areas into four larger regions: East Coast, West Coast, Panhandle, and Alabama/Georgia (Fig. 5). To minimize spatial discontinuities at the boundaries, the regions were permitted to overlap, and the probabilities for grid points within the overlapping regions were averaged.

The initial set of candidate predictors consisted of parameters calculated from the RUC analyses (Table 3), as well as the map type and climatological frequencies for each 3-h period. We performed a Principal Component Analysis (PCA) to examine inter-correlations among the predictors (Table 3) and to aid in choosing a smaller subset to retain for the regression analysis. This procedure is described in Shafer and Fuelberg (2006).

The final list of candidate predictors is given in Table 4. Also shown in Table 4 are Spearman rank correlation coefficients between each predictor and the binary indicator for one or more flashes during the 1800-2059 UTC period for the East Coast (EC) region. The correlations are low, meaning that no single observed predictor is a good indicator of lightning (Bothwell 2002; Shafer and Fuelberg 2006). Correlations for the amount of lightning (not shown) also were found to be low. To account for possible non-linear and interaction effects, power terms up to the fourth degree and two-way cross products were calculated for each parameter selected thus far (Table 4) and then included in the final predictor pool.

A combination of forward stepwise selection and cross-validation was used to develop the BLR equations for each region (Fig. 5) and 3-h period using the SPSS software. This procedure is very similar to that described in Shafer and Fuelberg (2006). Data for even numbered years were used as a "learning" sample for screening the variables for selection, while the odd years were used as an "evaluation" sample to test the model each time a variable was added or removed during the stepwise selection process. Thorough discussions of stepwise selection procedures are given in Hosmer and Lemeshow (1989) and Wilks (2006). The predictors comprising the model at the step with the highest percentage of correctly classified events for the evaluation sample were noted. Only parameters for which the sign of the coefficient made physical sense were retained in the model in any screening sample. This procedure identified the combination of predictors that is most likely to generalize to independent data and not over-fit the dependent sample. The set of "best" predictors from this process then was re-entered using data for all grid points and all years to determine the final coefficients for each model.

The NB models for PROB≥T were developed using S-PLUS. We found that the overnight and early morning periods did not contain a sufficient number of events in the upper percentiles to allow stable, reliable models to be developed. Thus, NB models were developed only for the four most active periods (1500-1759 UTC, 1800-2059 UTC, 2100-2359 UTC, and 0000-0259 UTC). The same sampling procedure (i.e., even and odd years) described above was used to develop the models. However, since the S-PLUS software does not permit stepwise selection for NB regression, a backward elimination procedure was used.

We used a model containing only climatology and persistence (denoted L-CLIPER) as the benchmark for assessing forecast skill. Climatology consisted of the lightning frequencies and unconditional means for each 3-h period (Section 3), as well as the sine of the day number. Persistence consisted of a binary indicator for whether one or more flashes occurred during the same 3-h period the previous day, as well as the previous day's flash count. Separate L-CLIPER models were developed for each region and 3-h period.

4. RESULTS

4.1 *Discussion of Model Parameters*

This section describes the parameters selected for the BLR and NB models as well as their relationships to lightning occurrence. The discussion focuses on the most active lightning period (1800-2059 UTC). However, since the equations for each 3-h period are variations on a similar theme, the physical reasoning presented here can be extended to all other times.

The BLR models giving PROB≥1 and the NB models for PROB≥T during the 1800-2059 UTC period are shown in Tables 5 and 6, respectively, for the four study regions (Fig. 5). The predictors and standardized coefficients are indicated. A series of diagrams displaying the frequency of one or more flashes (FREQ≥1) and the unconditional mean number of flashes (MEANNF) as a function of several important predictors is shown in Figs. 6-9. The acronyms used to describe the predictors are defined in Tables 3 and 4.

PRECPW is the most important predictor for one or more flashes (Table 5 and Fig. 6a), while KI, a measure of 850-700 hPa moisture as well as stability, was selected in 3 out of the 4 NB models estimating the amount of lightning (Table 6 and Fig. 6b). This finding agrees with numerous studies indicating that deep layer moisture provides the most favorable large-scale environment for warm season thunderstorms over Florida (e.g., Lopez et al. 1984; Reap and MacGorman 1989; Watson et al. 1995; Mazany et al. 2002). A non-linear effect also is evident for PRECPW (Fig. 6a), with a peak in FREQ≥1 for PRECPW ~ 5.5 cm, followed by a decline for even greater values.

BESTLI was selected as the second most important parameter in the BLR models (Table 5 and Fig. 7a) and also is important for predicting the amount of lightning (Table 6 and Fig. 7b). The negative coefficients and the relationships depicted in Fig. 7 imply that FREQ≥1 and MEANNF increase with increasing instability (i.e., as BESTLI becomes more negative). Many studies have shown that sufficient instability that leads to a persistent, strong updraft is necessary for charge generation (e.g., Price and Rind 1992; Solomon and Baker 1994; Zipser 1994; Petersen and Rutledge 1998).

Coincident areas of abundant moisture (PRECPW) and instability (BESTLI) are expected to be regions of high thunderstorm probability; however, storms will not develop without a source of lift. The selection of MFLXC2 in the BLR and NB models (Tables 5 and 6) indicates that boundary layer forcing is important for lightning formation (e.g., Watson et al. 1987; Reap and MacGorman 1989; Watson et al. 1991). The relationships in Figs. 8a-b show that FREQ≥1 and MEANNF generally increase with greater MFLXC2.

First and second-order terms of 1000-700 hPa mean wind (MEANU3, MEANV3) were selected in several equations (Tables 5 and 6). This relationship is non-linear for the EC region (Figs. 9a-b), with peak lightning for offshore speeds between 2 and 4 m s^{-1}, and a decline for increasing MEANU3. Weak offshore flow produces a better developed sea breeze and greater low level convergence, while strong offshore flow may prevent the sea breeze from penetrating inland (McPherson 1970; Pielke 1974; Arritt 1993). Interaction terms involving MEANU3 and the distance from the coast (DISTEC, DISTWC) also were selected, implying that this relationship is modulated by proximity to the coast.

Finally, the pattern type predictors (MTFREQ and MTMEAN) enter all of the equations (Tables 5 and 6). Although MTFREQ does not rank highly in the BLR models during the 1800-2059 UTC period, it usually is among the first selected for other time periods. Conversely, MTMEAN consistently is the most important predictor in the NB models, implying that the prevailing wind greatly influences locations where storms are most likely to persist over an area and produce large lightning counts (López and Holle 1987; Lericos et al. 2002).

4.2 *Reliability*

Reliability is a measure of the quality of probabilistic forecasts, indicating how well the probabilities correspond with the observed frequency of the predictand (Wilks 2006). Figure 10 plots FREQ≥1 as a function of PROB≥1 for all regions combined during the 1800-2059 UTC period. Similarly, Figs. 11a-d show reliability plots for forecasting the unconditional probability of exceeding the 50th, 75th, 90th, and 95th percentiles during the 1800-2059 UTC period (Table 1). Figs. 10 and 11 show that the forecasts exhibit good reliability and are well calibrated, meaning that the event relative frequencies are nearly identical to the forecast probabilities. Reliability at the other time periods (not shown) also is very good. Probabilistic verification and skill scores relative to climatology and persistence are presented next for the 2006 independent test period.

5. INDEPENDENT TEST PERIOD

5.1 *Description of model data*

We applied the lightning guidance equations (Section 4) to forecast output from two mesoscale models run by NCEP during the 2006 warm season and to output from local high resolution runs of the Weather Research and Forecasting (WRF) model for a domain over South Florida. The two NCEP models were the 1500 UTC run of the 13-km RUC (RUC13) and the 1200 UTC run of the 12-km North American Mesoscale (NAM12). The high resolution WRF runs were initialized at 1500 UTC with NCEP 1/12th degree sea-surface temperatures (SST) and data from the Local Analysis and Prediction System (LAPS).

A description of RUC's model physics and data assimilation methods can be found in Benjamin et al. (2002, 2004). We also used two versions of the WRF model to evaluate the lightning guidance equations—the 1200 UTC run of the 12-

km NCEP operational NAM-WRF and a 4-km LAPS-initialized WRF (WRF-LAPS) that is run locally at the NWS Weather Forecast Office (WFO) in Miami, FL. Janjic et al. (2004) and Skamarock et al. (2005) describe the physics and parameterization options for the WRF model.

WRF-LAPS is part of the WRF Environmental Modeling System (WRF-EMS) that is distributed by Dr. Robert Rozumalski at the University Corporation for Atmospheric Research (UCAR). Unlike the NCEP operational NAM-WRF, the version run at WFO Miami uses high resolution LAPS data for model initialization (see Hiemstra et al. 2006 for a description of LAPS). Etherton and Santos (2006) have documented the usefulness of LAPS data for local modeling.

WRF-LAPS forecasts (initialized at 1500 UTC) for the period 19-30 September 2006 were provided by Dr. Pablo Santos (NWS Miami, FL), while runs for the 1 August – 18 September 2006 period were produced locally at Florida State University (FSU) using the WRF-EMS package. The LAPS, 1/12th degree SST, and NAM12 lateral boundary condition files that were required to produce the FSU runs were provided by Dr. Santos. The WRF-LAPS domain is centered on the Miami WFO county warning area (Fig. 1).

Forecasts from RUC13 encompass the entire 2006 warm season (1 May – 30 September), while forecasts from the NCEP operational NAM-WRF span 21 June – 30 September (the NAM-WRF became operational on 20 June). We used forecasts valid every 3 h out to 12 h (i.e., the 0-h, 3-h, 6-h, 9-h, and 12-h projections). Forecast parameters needed for the lightning guidance equations were calculated from the model forecast temperature, dew point, wind, height, and surface pressure fields and interpolated to the 10 × 10-km forecast grid (Fig. 1).

5.2 *Forecast verification*

The most commonly used measure of accuracy for probabilistic forecasts is the Brier score (Brier 1950) given by:

$$BS = \frac{1}{N}\sum_{i=1}^{N}\left(f_i - o_i\right)^2 \quad , \qquad (7)$$

where N is the number of forecast-observation pairs (i.e., the number of grid points), f_i is the forecast probability, and o_i is the observation (set to 1 if the event occurred, or 0 if the event did not occur). Perfect forecasts exhibit BS = 0, while less accurate forecasts have 0 < BS ≤ 1. We also calculated the Brier Skill Score, given by:

$$BSS = 1 - \frac{BS_{MODEL}}{BS_{REF}} \quad , \qquad (8)$$

where BS_{MODEL} is the Brier score for the model and BS_{REF} is the Brier score for a reference forecast (i.e., L-CLIPER). It is clear from (8) that forecasts with a lower Brier score than the reference will have BSS > 0 (positive skill), while forecasts with higher Brier scores than the reference have BSS < 0 (negative skill).

Brier scores for forecasting the probability of one or more CG flashes during each 3-h period are shown in Table 7 for the 1200 UTC NCEP NAM12 (top), the 1500 UTC NCEP RUC13 (middle), and the 1500 UTC WRF-LAPS (bottom). The rightmost column shows the Brier skill score with respect to L-CLIPER (left) and persistence alone (right). Results show that Brier scores are smallest for the less active time periods, and greatest for the more active periods (i.e., 1800-2359 UTC). This occurs because Brier scores tend to be lower when the variance of the forecasts and observations is small (i.e., little lightning and small probabilities), and vice versa when the variance of forecasts and observations is large (Burrows et al. 2005). More importantly, Brier scores for all three models generally are an improvement over L-CLIPER and an even greater improvement over persistence alone through the 2100-2359 UTC period. It is important to note that results for the different models should not be compared with each other since they are from different initialization times (for the NAM12) and represent different time periods and different regions of the state.

Forecasting the amount of lightning is much more difficult than forecasting whether or not at least one flash will occur. Table 8 shows Brier scores and Brier skill scores for forecasting events in the 75th percentile of flashes or greater (Table 1), conditional on the occurrence of one or more flashes. Results show that Brier scores generally are higher, and skill scores relative to L-CLIPER and persistence generally are lower than those for merely forecasting one or more flashes (Table 7). Nonetheless, skill scores generally are positive through the 2100-2359 UTC period. For events in the 90th percentile or greater (not shown), Brier skill scores are slightly positive or near zero at

most time periods, with only the RUC13 producing positive skill through the 2100-2359 UTC period. This finding suggests that events in the 90th or greater percentiles are near the threshold of predictability, at least for forecasts longer than 3-6 h. This is likely due to an inherent weakness in the PP method, namely, the tendency to forecast extreme events unreliably when the accuracy of the predictors (i.e., the NWP model forecasts) decreases to the point where it is inadvisable to attempt to predict the extremes of the distribution (Glahn et al. 1991).

The Brier score computations (Tables 8 and 9) require that lightning events occur within a 10-km radius of a grid point. This is a very strict verification criterion that does not consider forecasts at neighboring grid points. A more relaxed approach is to use the maximum probability or the average probability within a certain radius of each grid point (e.g., Burrows et al. 2005). The maximum or average probability then is used in the Brier Score computations instead of the grid point specific values. We determined that maximum probabilities within 20 km of each grid point generally give the best improvement relative to L-CLIPER and persistence. The results using this new verification approach are shown in Tables 9 and 10 for forecasting one or more flashes and forecasting events in the 75th percentile or greater, respectively. In most cases, magnitudes of the Brier scores remain relatively unchanged; however, Brier skill scores generally are higher when using the more relaxed verification criteria, especially during the first 6 h of the forecast. For reasons that are not clear, the relaxed criteria most benefit L-CLIPER and persistence during the later forecast periods (as evident by the lower skill scores for these periods in Table 9 and 10).

As one would expect, skill scores deteriorate beyond the 6-9 h projections (Tables 8-11) since errors in the position and magnitude of predicted convection and synoptic scale features increase with time in the driving NWP models. Nonetheless, the results in Tables 8-11 are encouraging, especially considering that L-CLIPER alone generally produces very good forecasts during Florida's warm season. In fact, L-CLIPER is the most difficult standard of reference to beat since it represents an optimal linear combination of both climatology and previous day persistence. L-CLIPER becomes particularly difficult to beat in situations when the synoptic pattern on a particular day is similar to that of the previous day, which often is the case during Florida's warm season.

Figures 12 and 13 contain reliability diagrams for forecasting the probability of one or more flashes and the probability of $\geq$ 75th percentile events, respectively, for the most active lightning period (1800-2059 UTC). Results for the three mesoscale models are plotted on the same graph. Forecasts from RUC13 lie reasonably close to the 1:1 line in both plots. However, forecasts for the NAM12 and WRF-LAPS show an under-forecasting bias in the lower half of the probability range, and then bend back toward the 1:1 line at higher forecast probabilities. The reason for this behavior is not entirely clear, but most likely is due to inherent biases in the model moisture, temperature, and/or wind field forecasts. Reliability plots for other forecast projections (not shown) indicate similar biases. Reliability when forecasting the 90th percentile or greater (not shown) is similar to that for the 75th percentile (Fig. 13), but tends to deviate a bit more from the 1:1 line for higher forecast probabilities.

5.3 *Forecast example*

An example lightning probability forecast for 16-17 August 2006 using the 1500 UTC WRF-LAPS model (Fig. 14) is described next. A map containing county names and labeled geographical features is shown in Fig. 15. Results using the RUC13 and NAM-WRF on this day (not shown) compare favorably with those from WRF-LAPS (Fig. 14). The figure shows the probability of one or more flashes (left panels), the unconditional probability of $\geq$ 90th percentile events (center), and the CG strike verification (right panels) for four 3-h time periods. The flow pattern on this day is type A (Section 3), with prevailing southeasterly low-level flow and no synoptic or tropical influences. Between 1500-1759 UTC, the greatest probability of one or more flashes (between 30-40%) is forecast over eastern Broward and northern Miami-Dade (MD) counties, with probabilities of 10% or greater for areas south of Lake Okeechobee (LOK) (Fig. 14a). Forecast probabilities beginning at 1800 UTC (Figs. 14d and e) are considerably greater than those at 1500 UTC across South Florida (Figs. 14a and b), with the greatest values concentrated along the west coast as well as eastern PB, Broward, and MD counties. The verification (Fig. 14f) reveals a significant increase in activity (over 7000 flashes) along the west coast and over Broward and MD counties. With the exception of the activity south of LOK, this verification agrees well with the forecast probabilities (Figs. 14d and e). Forecast probabilities for the 2100-2359 UTC period (Figs. 14g and h) have

increased south of LOK, and lightning occurs just east of this area over central and western PB and Broward counties (Fig. 14i). Although the area of enhanced probabilities north of LOK does not verify during this period (Fig. 14i), lightning did occur there only one hour earlier, i.e., between 2000-2030 UTC (Fig. 14f). Finally, forecast probabilities for the 0000-0259 UTC period (Figs. 14j and k) show a diminishing lightning threat, and indeed little activity occurs during this period (Fig. 14l).

The example in Fig. 14 is typical of many others during the 1 August – 30 September 2006 period. That is, the sequence of probability maps shows the expected diurnal trend in lightning that peaks during the afternoon and then diminishes. The lightning forecasts generally show good agreement with the verification, with most of the observed lightning occurring within the higher forecast probability contours. However, as observed on 16-17 August, the timing and placement of lightning is not perfect. Nonetheless, the forecasts do capture the general spatial and temporal trends in observed lightning at a level of detail that, to our knowledge, has not been reported previously.

6. SUMMARY AND CONCLUSIONS

Four warm seasons of NLDN data and an archive of RUC20 analyses were used to develop forecast equations for the probability of one or more CG strikes, as well as the probability of exceeding various flash count percentile thresholds at 3-h periods on a 10×10 km grid. Binary logistic regression (BLR) and negative binomial (NB) regression were used to develop the equations for one or more flashes and the amount of lightning, respectively. Deep layer moisture, instability, boundary layer forcing, map type, and the low-level wind were found to be the most important predictors for lightning.

The equations were applied to forecast output from three mesoscale models during the period 1 May – 30 September 2006: the 1500 UTC NCEP RUC13, the 1200 UTC NCEP NAM-WRF, and high resolution runs of the WRF initialized at 1500 UTC with LAPS and NCEP 1/12th degree SST data (WRF-LAPS). When forecasting one or more flashes, all three mesoscale models generally showed positive skill relative to L-CLIPER and persistence alone through the 2100-2359 UTC period. Skill was found to deteriorate beyond 6-9 h as errors in the model forecasts increased with time in the driving NWP models. The models also showed some improvement over L-CLIPER and persistence when forecasting events in the 75th or greater percentiles, with limited skill for events in the 90th or greater percentiles. The positive skill demonstrated by the RUC13, NAM-WRF and WRF-LAPS (through 2100-2359 UTC) during the 1 May – 30 September 2006 test period provides some evidence that the PP scheme is model independent. Testing on a larger independent sample (i.e., multiple warm seasons) is needed to further support this hypothesis.

The guidance that we have developed represents an important step toward more precise and timely lightning forecasts. Our results indicate that skillful lightning forecasts out to 6-9 h are possible using high-resolution models. In addition, a major strength of the PP method is that the inevitable changes that will occur in the NWP models will not require redevelopment of the equations, and in fact, should improve the forecasts (Wilks 2006). Conversely, the main drawback is that the PP scheme assumes a "perfect" forecast/analysis of the predictors by the NWP model and thus, does not account for, or correct any type of NWP forecast error. Thus, it appears that some kind of MOS procedure would be needed to produce skillful forecasts beyond 9-12 h. Nonetheless, as model resolution, physics, and data assimilation methods continue to improve, better lightning forecasts are expected to result.

Our methodology is an enhancement to schemes already in use (e.g., Bothwell 2002, 2005). Further improvements will be achieved through additional research. Plans currently are in place to incorporate the lightning guidance into the Interactive Forecast Preparation System (IFPS) Graphical Forecast Editor (GFE) at the Tallahassee NWS office. A forecaster then can use output from one NWP model or a blend of two or more models to generate lightning probabilities using a "smart tool" in GFE. The resulting lightning forecasts then could be accessed by the public through NWS web sites and used by the NWS in forecast products. Future work also will seek to expand the scheme to other parts of the country. Since some of the statistical assumptions made for Florida may not be applicable to other areas, appropriate modifications likely will be needed.

Acknowledgements: This research was funded by Florida Power & Light Corporation (FP&L). We appreciate the assistance of Drs. James Elsner and Thomas Jagger of the Department of Geography at Florida State University for their helpful

suggestions and advice. Appreciation also is extended to Dr. Pablo Santos (NWS Miami) for providing the initialization datasets required to produce the WRF runs. We also wish to thank Paul Hebert from FP&L for providing many suggestions based on his extensive knowledge of summertime sea-breeze weather patterns in Florida.

REFERENCES

Arritt, R. W., 1993: Effects of the large-scale flow on characteristic features of the sea breeze. *J. Appl. Meteor*., **32**, 116-125.

Benjamin, S. G., J. M. Brown, K. J. Brundage, D. Devenyi, G. A. Grell, D. Kim, B. E. Schwartz, T. G. Smirnova, T. L. Smith, and S. S. Weygandt, 2002: RUC20- The 20-km version of the Rapid Update Cycle. *NWS Technical Procedures Bulletin*, No. 490, 30 pp.

-----, G. A. Grell, J. M. Brown, and T. G. Smirnova, 2004: Mesoscale weather prediction with the RUC hybrid isentropic-terrain-following coordinate model. *Mon. Wea. Rev*., **132**, 473-494.

Bothwell, P. D., 2002: Prediction of cloud-to-ground lightning in the western United States, Ph.D., University of Oklahoma, 178 pp.

Brier, G. W., 1950: Verification of forecasts expressed in terms of probability. *Mon. Wea. Rev*., **78**, 1-3.

Burrows, W. R., C. Price, and L. J. Wilson, 2005: Warm season lightning probability prediction for Canada and the northern United States. *Wea. Forecasting*, **20**, 971-988.

Camp, J. P., A. I. Watson, and H. E. Fuelberg, 1998: The diurnal distribution of lightning over north Florida and its relation to the prevailing low-level flow. *Wea. Forecasting*, **13**, 729-739.

Cummins, K. L., M. J. Murphy, E. A. Bardo, W. L. Hiscox, R. B. Pyle, and A. E. Pifer, 1998: A combined TOA/MDF technology upgrade of the U.S. National Lightning Detection Network. *J. Geophys. Res*., **103**, 9035-9044.

Elsner, J. B. and C. P. Schmertmann, 1993: Improving extended-range seasonal predictions of intense Atlantic hurricane activity. *Wea. Forecasting*, **8**, 345-351.

-----, J. B. and T. H. Jagger, 2004: A hierarchical Bayesian approach to seasonal hurricane modeling. *J. Climate*., **17**, 2813–2827.

Etherton, B., and P. Santos, 2006: Sensitivity of WRF forecasts for South Florida to initial conditions. Submitted to *Wea. Forecasting*.

Falls, L. W., W. O. Williford, and M. C. Carter, 1971: Probability distributions for thunderstorm activity at Cape Kennedy, Florida. *J. Appl. Meteor*., **10**, 97-104.

Gardner, W., E. P. Mulvey, and E. C. Shaw, 1995: Regression analysis of counts and rates: Poisson, overdispersed Poisson, and negative binomial models. *Psychological Bulletin*, **118**, No. 3, 392-404.

Glahn, H. R., and D. A. Lowry, 1972: The use of Model Output Statistics (MOS) in objective weather forecasting. *J. Appl. Meteor*., **11**, 1203-1211.

-----, A. H. Murphy, L. J. Wilson, and J. S. Jensenius, Jr., 1991: Lectures presented at the WMO training workshop on the interpretation of NWP products in terms of local weather phenomena and their verification, Wageningen, The Netherlands, 29 July-9 August 1991. WMO/TD. No. 421.

Hodanish, S., D. Sharp, W. Collins, C. Paxton, and R. E. Orville, 1997: A 10-year monthly lightning climatology of Florida: 1986-95. *Wea. Forecasting*, **12**, 439-448.

Hosmer, D. W., and S. Lemeshow, 1989: *Applied Logistic Regression*. John Wiley & Sons, Inc., 307 pp.

Hughes, K. K., 2001: Development of MOS thunderstorm and severe thunderstorm forecast equations with multiple data sources. Preprints, *18th Conf. on Weather Analysis and Forecasting*, Fort Lauderdale, FL, Amer. Meteor. Soc., 191-195.

Janjic, Z., T. Black, M. Pyle, H. Chuang, E. Rogers, and G. DiMego, 2004: *An Evolu-*

tionary Approach to Non-Hydrostatic Modeling. Available [http://www.wrf-model.org].

Klein, W. H., 1971: Computer prediction of precipitation probability in the United States. *J. Appl. Meteor*., **10**, 903-915.

-----, B. M. Lewis, and I. Enger, 1959: Objective prediction of five day mean temperature during winter. *J. Meteor*., **16**, 672-682.

Laird, N. F., D. A. R. Kristovich, R. M. Rauber, H. T. Ochs III, and L. J. Miller, 1995: The Cape Canaveral sea and river breezes: kinematic structure and convective initiation. *Mon. Wea. Rev*., **123**, 2942-2956.

Lambert, W. C., M. Wheeler, and W. Roeder, 2005: Objective lightning forecasting at Kennedy Space Center and Cape Canaveral Air Force Station using cloud-to-ground lightning surveillance system data. *Preprints, Conference on Meteorological Applications of Lightning Data*, San Diego, CA, Amer. Meteor. Soc.

Lehmiller, G. S., T. B. Kimberlain, and J. B. Elsner, 1997: Seasonal prediction models for North Atlantic basin hurricane location. *Mon. Wea. Rev*., **125**, 1780-1791.

Lericos, T. P., H. E. Fuelberg, A. I. Watson, and R. L. Holle, 2002: Warm season lightning distributions over the Florida peninsula as related to synoptic patterns. *Wea. Forecasting*, **17**, 83-98.

Livingston, E. S., J. W. Nielson-Gammon, and R. E. Orville, 1996: A climatology, synoptic assessment, and thermodynamic evaluation for cloud-to-ground lightning in Georgia: A study for the 1996 Summer Olympics. *Bull. Amer. Meteor. Soc*., **77**, 1483-1495.

López, R. E., P. T. Gannon, Sr., D. O. Blanchard, and C. C. Balch, 1984: Synoptic and regional circulation parameters associated with the degree of convective shower activity in South Florida. *Mon. Wea. Rev*., **112**, 686-703.

-----, and R. L. Holle, 1987: The distribution of summertime lightning as a function of low-level wind flow in central Florida. NOAA Tech. Memo. ERL ESG-28, National Severe Storms Laboratory, Norman, OK, 43 pp.

Lund, I. A., 1963: Map-pattern classification by statistical methods. *J. Appl. Meteor*., **2**, 56-66.

Mazany, R. A., Businger, S., Gutman, S. I., and Roeder, W., 2002: A lightning prediction index that utilizes GPS integrated precipitable water vapor. *Wea. Forecasting*, **17**, 1034-1047.

McPherson, R. D., 1970: A numerical study of the effect of a coastal irregularity on the sea breeze. *J. Appl. Meteor*., **9**, 767-777.

Neumann, C. J., and J. R. Nicholson, 1972: Multivariate regression techniques applied to thunderstorm forecasting at the Kennedy Space Center. *Preprints, International Conference on Aerospace and Aeronautical Meteorology*, Washington, D.C., Amer. Meteor. Soc., 6-13.

Orville, R. E., 1994: Cloud-to-ground lightning flash characteristics in the contiguous United States: 1989-1991. *J. Geophys. Res*., **99**, 10 833-10 841.

-----, and G. R. Huffines, 2001: Cloud-to-ground lightning in the United States: NLDN results in the first decade, 1989-98. *Mon. Wea. Rev*., **129**, 1179-1193.

-----, G. R. Huffines, W. R. Burrows, R. L. Holle, and K. L. Cummins, 2002: The North American Lightning Detection Network (NALDN)—first results: 1998-2002. *Mon. Wea. Rev*., **130**, 2098-2109.

Petersen, W. A., and S. A. Rutledge, 1998: On the relationship between cloud-to-ground lightning and convective rainfall. *J. Geophys. Res*., **103**, 14025-14040.

Pielke, R. A., 1974: A three-dimensional numerical model of the sea breezes over south Florida. *Mon. Wea. Rev*., **102**, 115-139.

Price, C., and D. Rind, 1992: A simple lightning parameterization for calculating global lightning distributions. *J. Geophys. Res*., **97**, 9919-9933.

Reap, R. M., 1994: Analysis and prediction of lightning strike distributions associated with synoptic map types over Florida. *Mon. Wea. Rev*., **122**, 1698-1715.

-----, and D. S. Foster, 1979: Automated 12-36 hour probability forecasts of thunderstorms and severe local storms. *J. Appl. Meteor*., **18**, 1304-1315.

-----, and D. R. MacGorman, 1989: Cloud-to-ground lightning: climatological characteristics and relationships to model fields, radar observations, and severe local storms. *Mon. Wea. Rev*., **117**, 518-535.

Reynolds, S. E., M. Brook, and M. F. Gourley, 1957: Thunderstorm charge separation. *J. Meteorol*., **14**, 426-436.

Sakamoto, C. M, 1973: Application of the Poisson and Negative Binomial models to thunderstorm and hail days probabilities in Nevada. *Mon. Wea. Rev*., **101**, 350-355.

Shafer, P. E., and H. E. Fuelberg, 2006: A statistic cal procedure to forecast warm season lightning over portions of the Florida peninsula. *Wea. Forecasting*, **21**, 851-868.

-----, and H. E. Fuelberg, 2007: A perfect prognosis scheme for forecasting warm season lightning over Florida. Accepted by *Mon. Wea. Rev.*

Skamarock, W. C., J. B. Klemp, J. Dudhia, D. O. Gill, D. M. Barker, W. Wang, and J. G. Powers, 2005: A description of the Advanced Research WRF Version 2. NCAR Tech Notes-468+STR. Available [http://www.mmm.ucar.edu/wrf/urs/docs/arw_v2.pdf].

Solomon, R., and M. Baker, 1994: Electrification of New Mexico thunderstorms. *Mon. Wea. Rev*., **122**, 1878-1886.

Steiger, S. M., R. E. Orville, and G. Huffines, 2002: Cloud-to-ground lightning characteristics over Houston, Texas: 1989-2000. *J. Geophys. Res*., **107**, D11,10.1029/ 2001 JD001142.

Vonnegut, B., 1963: Some facts and speculations concerning the origin and role of thunderstorm electricity. *Meteorol. Monogr*., **5**, 224-241.

Watson, A. I., R. E. López, R. L. Holle, and J. R. Daughetry, 1987: The relationship of lightning to surface convergence at Kennedy Space Center: A preliminary study. *Wea. Forecasting*, **2**, 140-157.

-----, R. L. Holle, R. E. López, R. Ortiz, and J. R. Nicholson, 1991: Surface wind convergence as a short-term predictor of cloud-to-ground lightning at Kennedy Space Center. *Wea. Forecasting*, **6**, 49-64.

-----, R. L. Holle, and R. E. López, 1995: Lightning from two national detection networks related to vertically integrated liquid and echo-top information from WSR-88D radar. *Wea. Forecasting*, **10**, 592-605.

Westcott, N. E., 1995: Summertime cloud-to-ground lightning activity around major Midwestern urban areas. *J. Appl. Meteor*., **34**, 1633-1642.

Wilks, D. S., 2006: Statistical Methods in the Atmospheric Sciences. International Geophysics Series, Vol. 91, Academic Press, 627 pp.

Williams, E. R., 1985: Large-scale charge separation in thunderclouds. *J. Geophys. Res*., **90**, 6013-6025.

-----, M. E. Weber, R. E. Orville, 1989: The relationship between lightning type and convective state of thunderclouds. *J. Geophys. Res*., **94**, 13213-13220.

Williford, W. O., M. C. Carter and P. Hsieh, 1974: A Bayesian analysis of two probability models describing thunderstorm activity at Cape Kennedy, Florida. *J. Appl. Meteor*., **13**, 718-725.

Zipser, E. J., 1994: Deep cumulonimbus cloud systems in the tropics with and without lightning. *Mon. Wea. Rev*., **122**, 1837-1851.

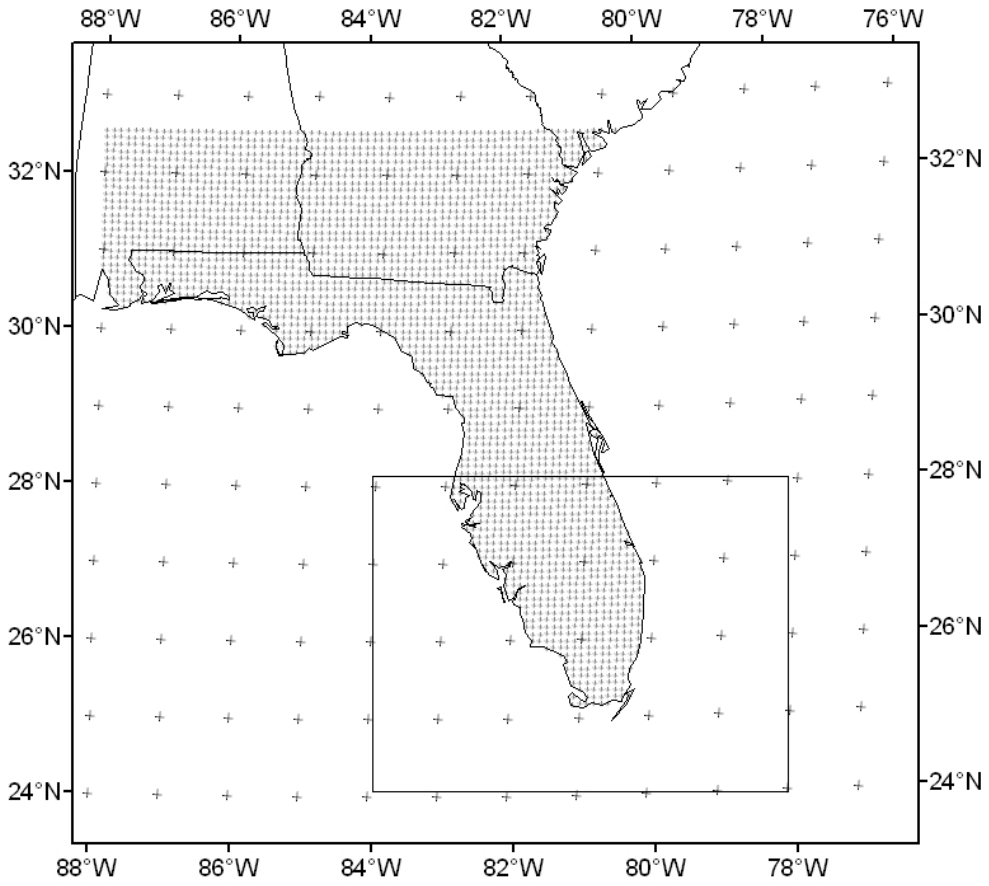

FIG. 1. Map of the study domain. The 10 km grid points used in equation development (land areas only) and the array of 100 km grid points used in the map type classification analysis are shown. The WRF-LAPS computational domain (South Florida) also is indicated by the rectangle.

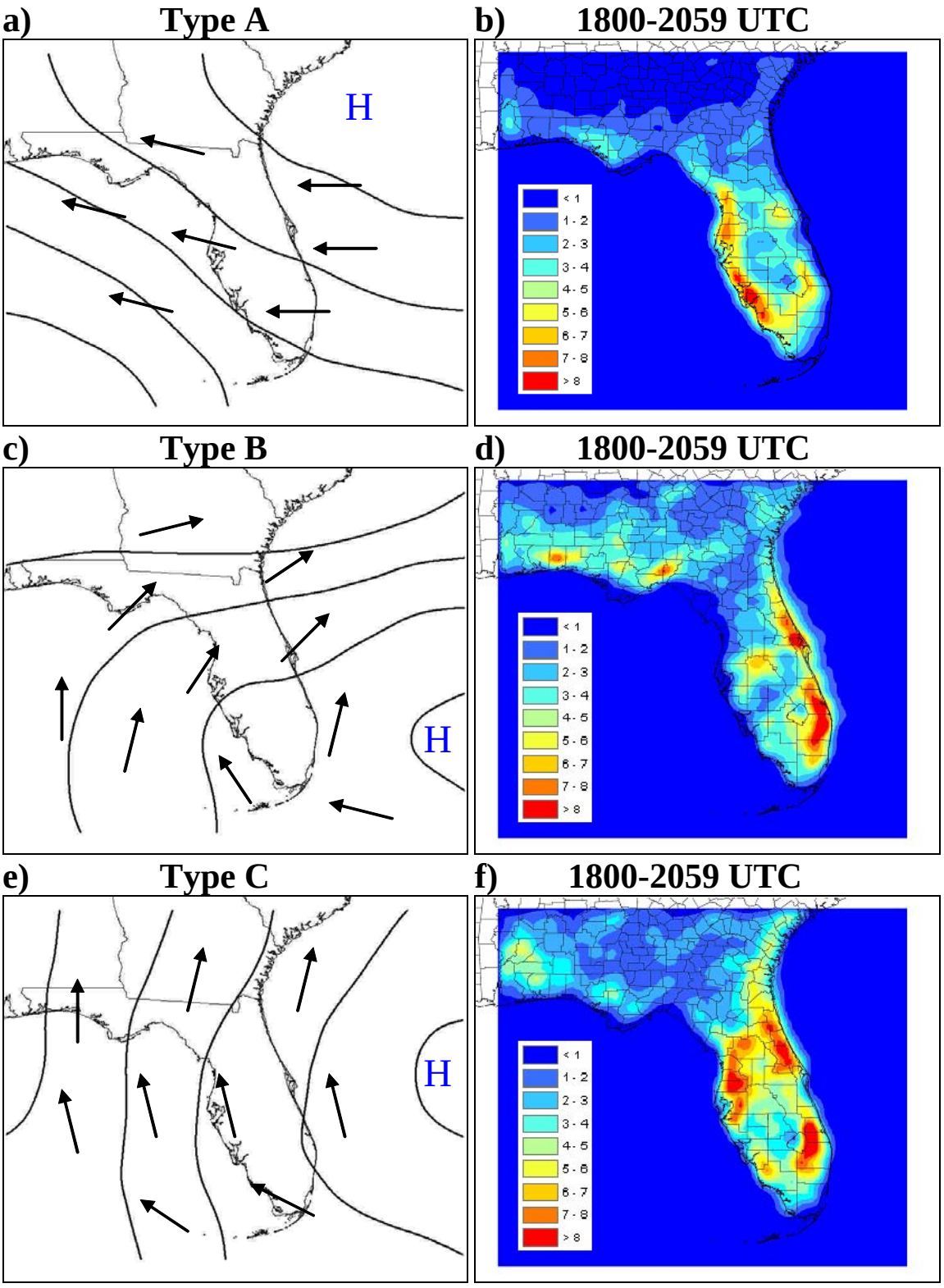

FIG. 2. Composite sea level pressure and spatial distribution of the unconditional mean number of flashes for the 1800-2059 UTC period for (a-b) type A, (c-d) type B, (e-f) type C, (g-h) type D, and (i-j) type E. The inferred low-level wind is indicated by arrows on each map.

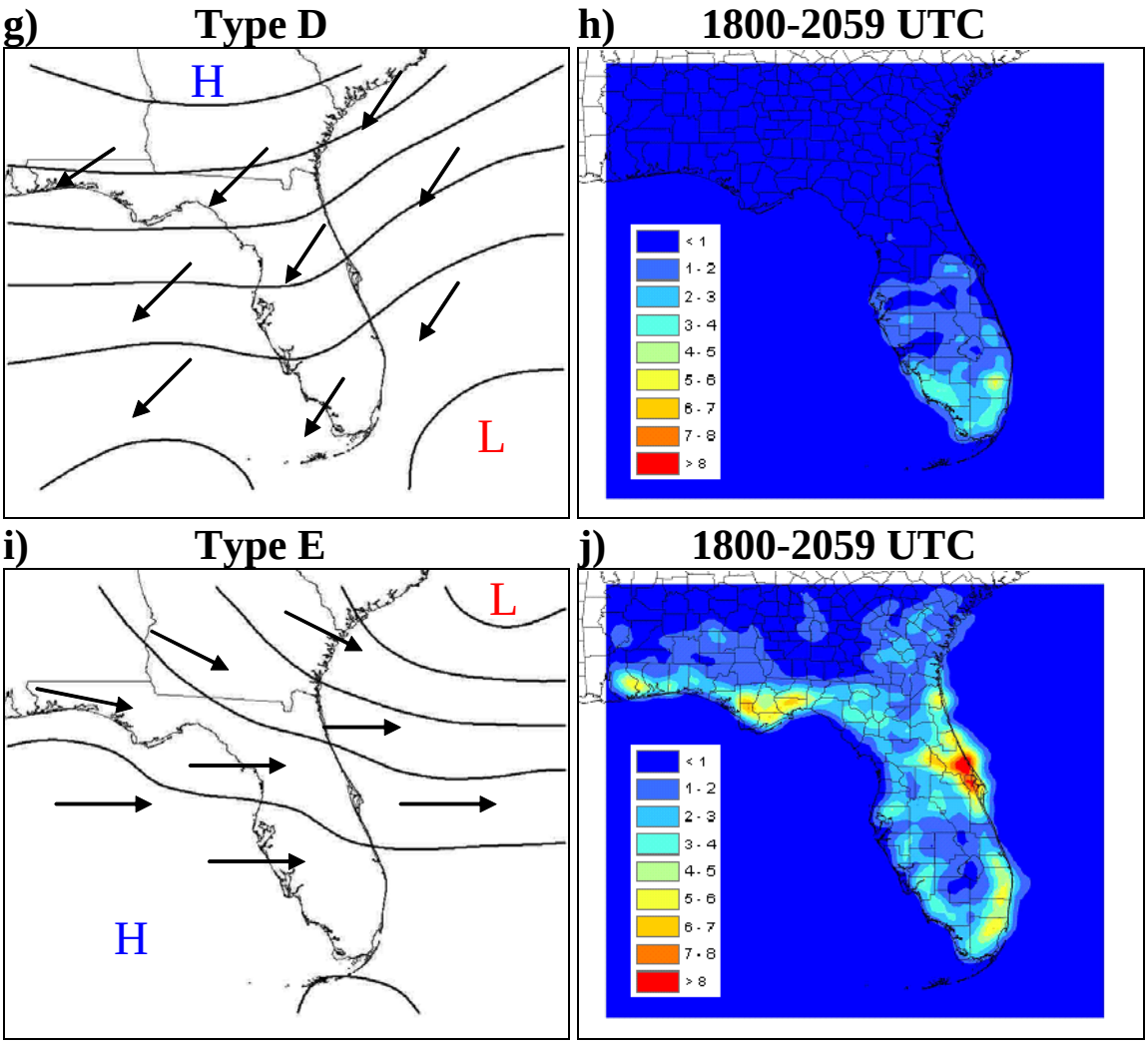

FIG. 2 (continued).

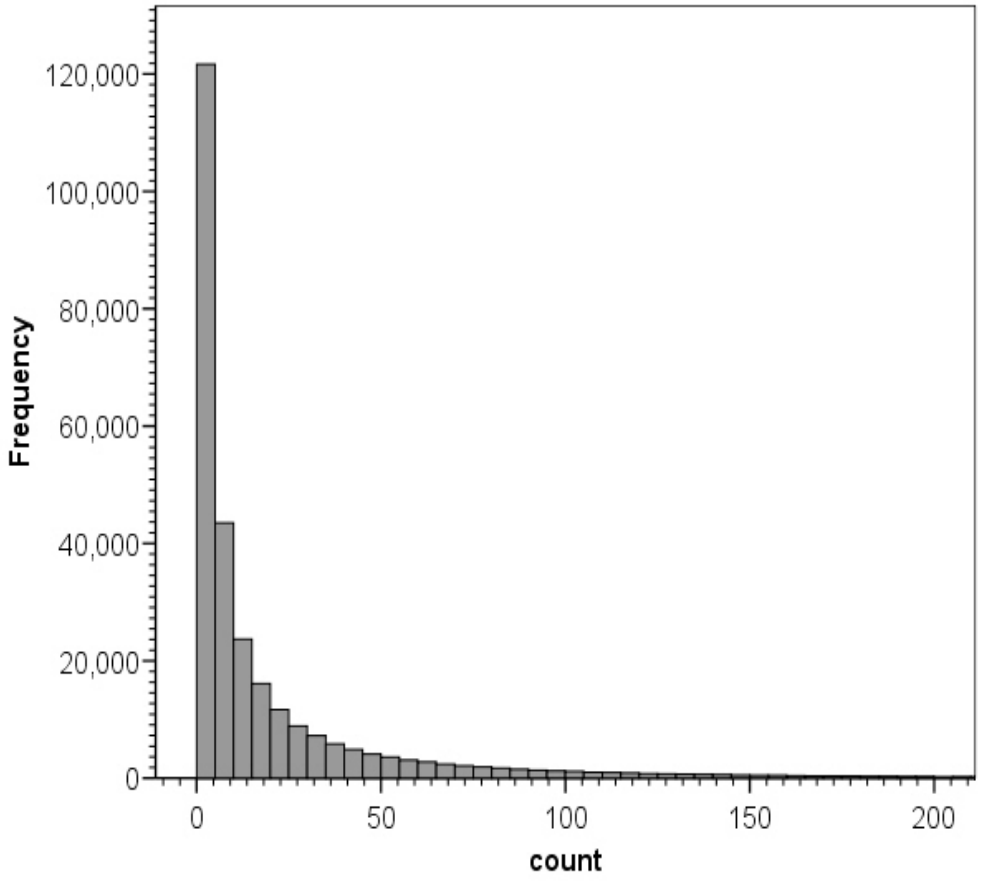

FIG. 3. Histogram of the distribution of flash counts during the 1800-2059 UTC period for all cases when one or more flashes occurred. The histogram has been truncated at 200 flashes to emphasize the lower part of the distribution. Histogram bins are 5 flashes.

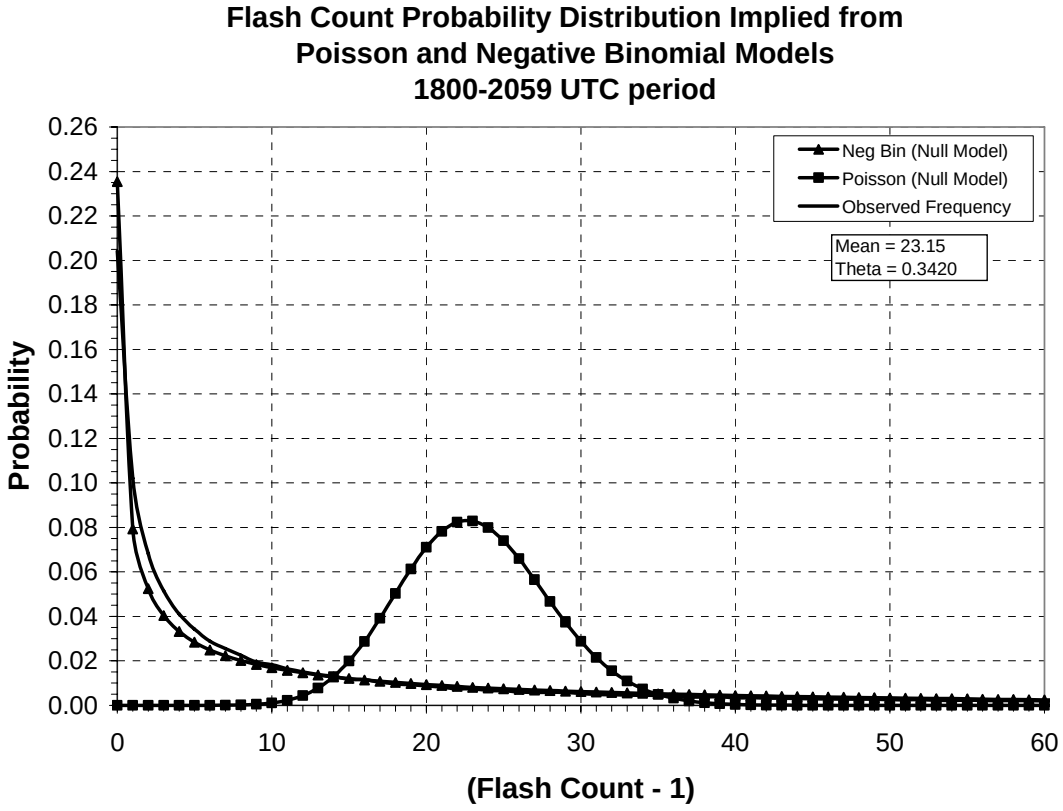

FIG. 4. Flash count probability distribution for the 1800-2059 UTC period implied from the Poisson and negative binomial regression models. The observed frequency also is shown for comparison.

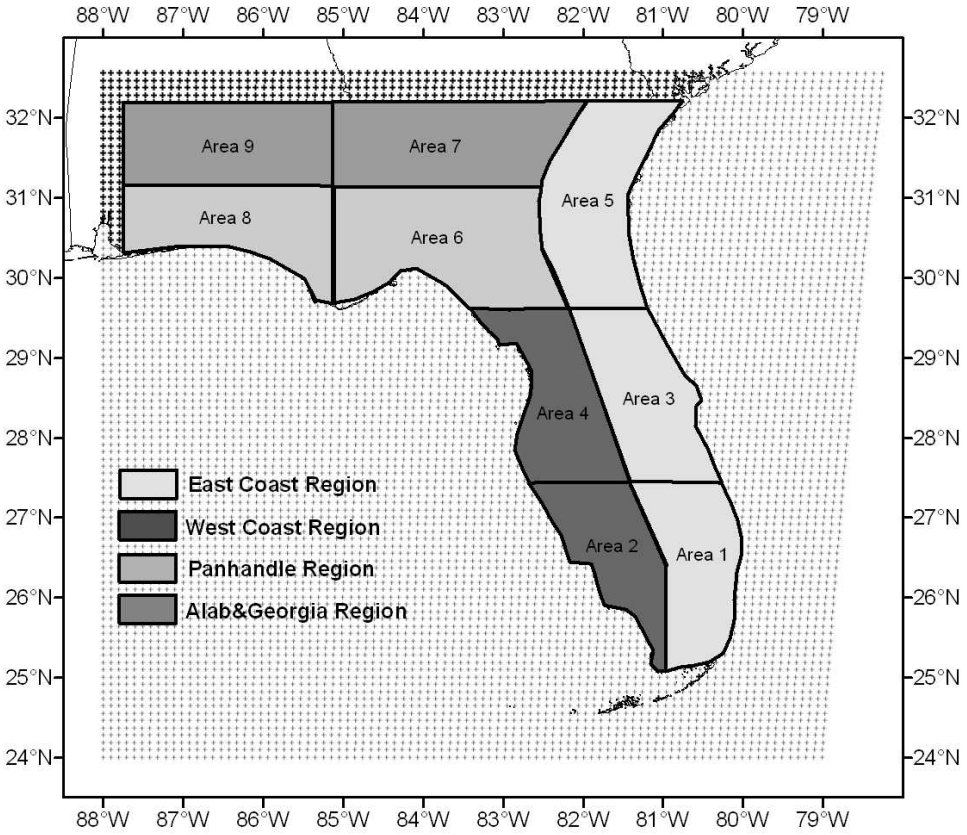

FIG. 5. Map of the original nine areas for which equations first were developed. The shaded areas represent the final four regions used to develop equations.

a)

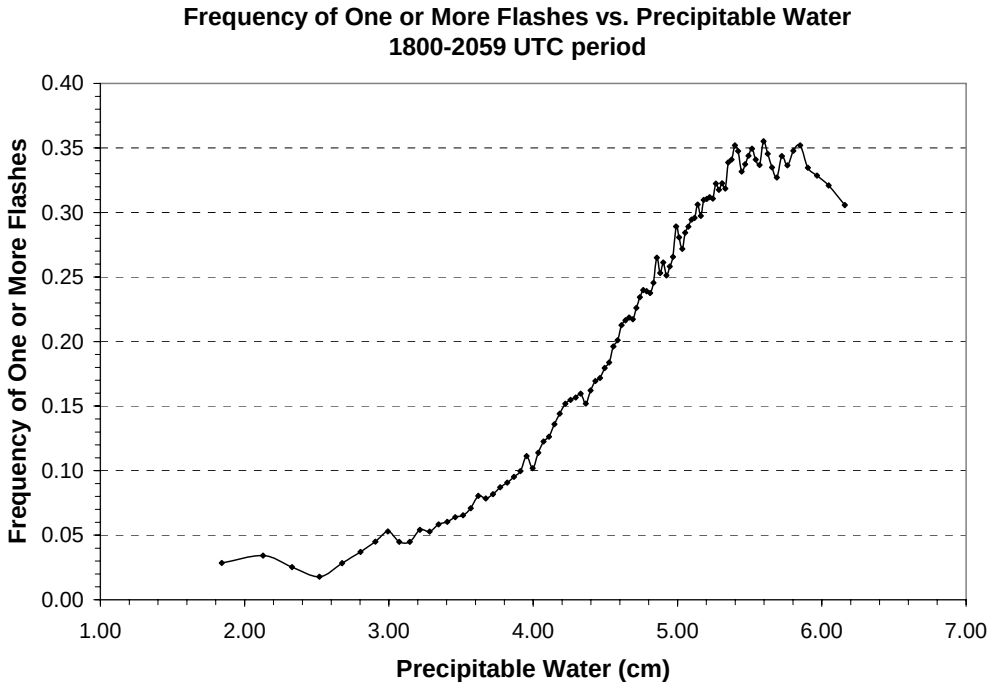

b)

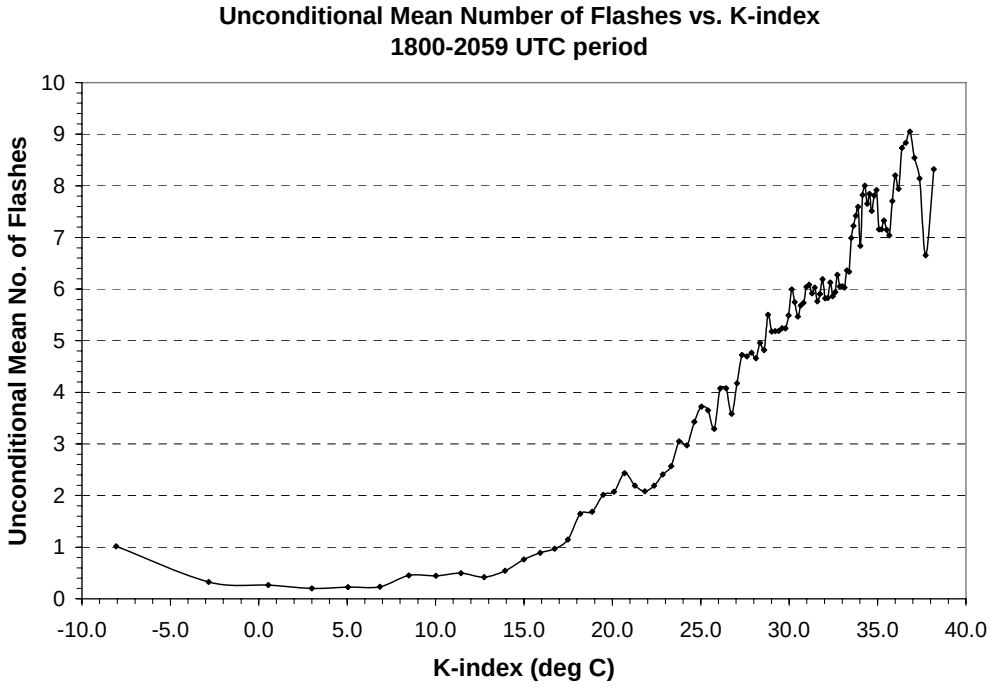

FIG. 6**.** Plots for a) the frequency of one or more flashes as a function of precipitable water, and b) the unconditional mean number of flashes as a function of K-index for all regions combined during the 1800-2059 UTC period.

a)

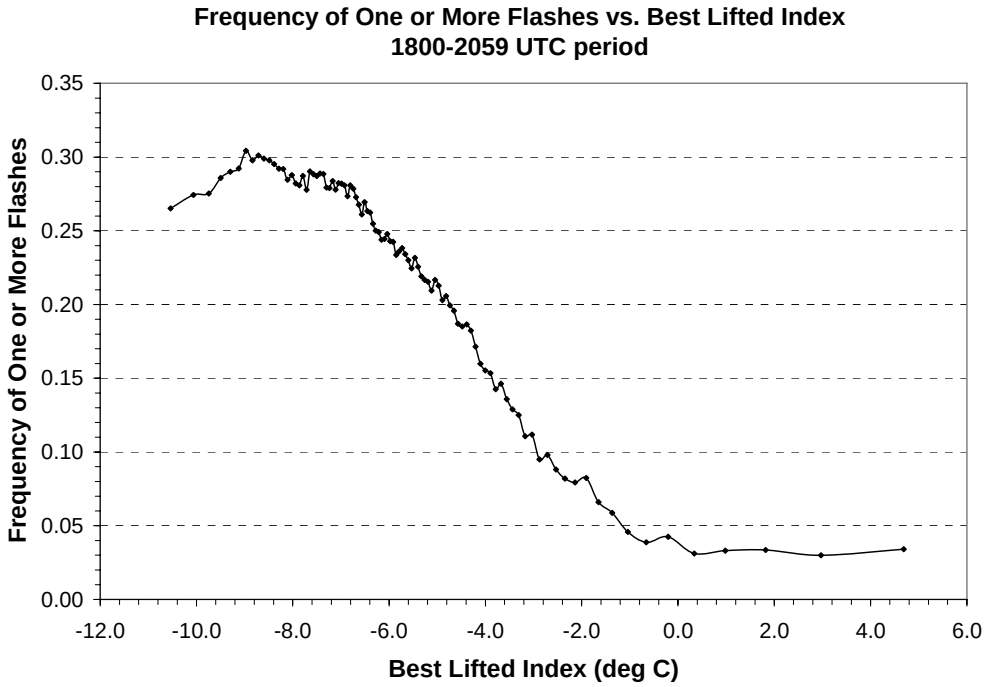

b)

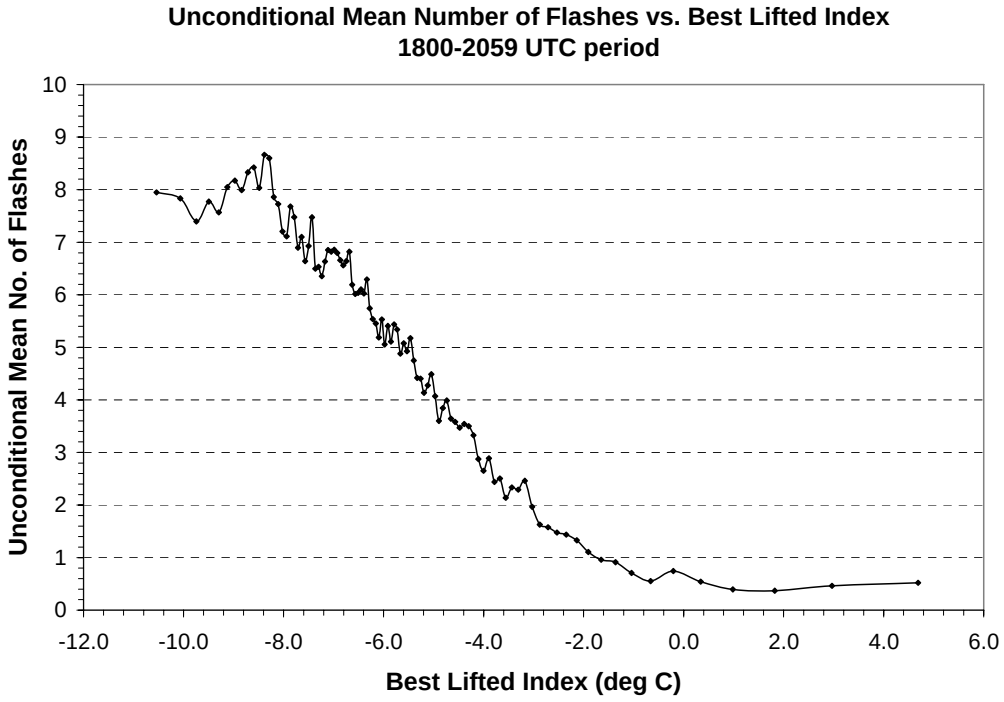

FIG. 7. Plots for a) the frequency of one or more flashes as a function of Best Lifted Index, and b) the unconditional mean number of flashes for all regions combined during the 1800-2059 UTC period.

a)

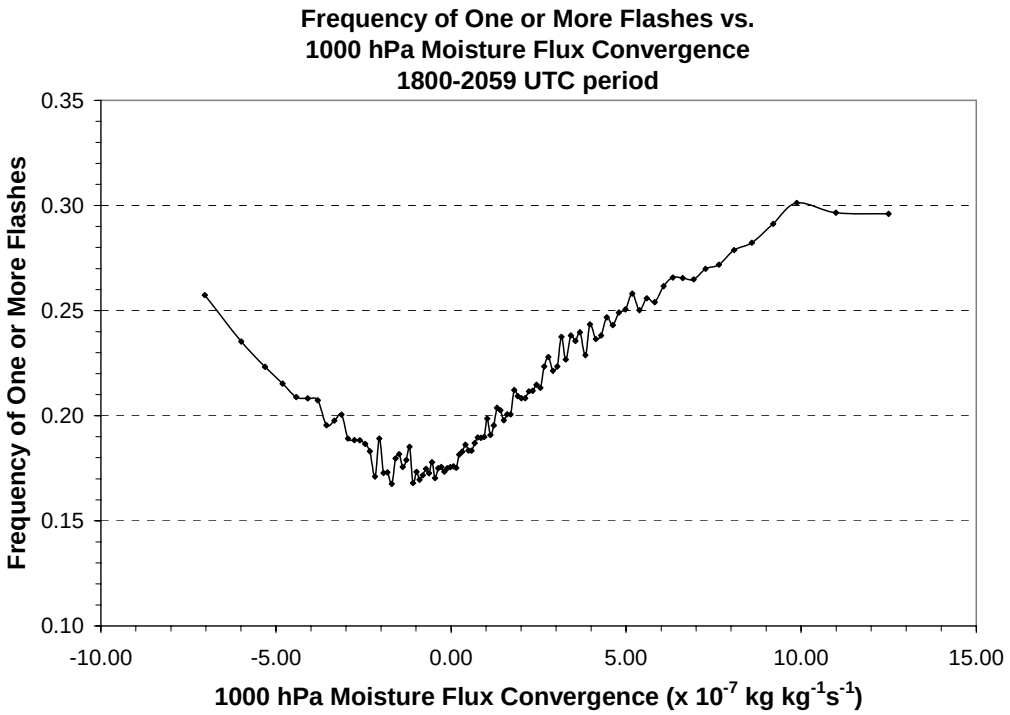

b)

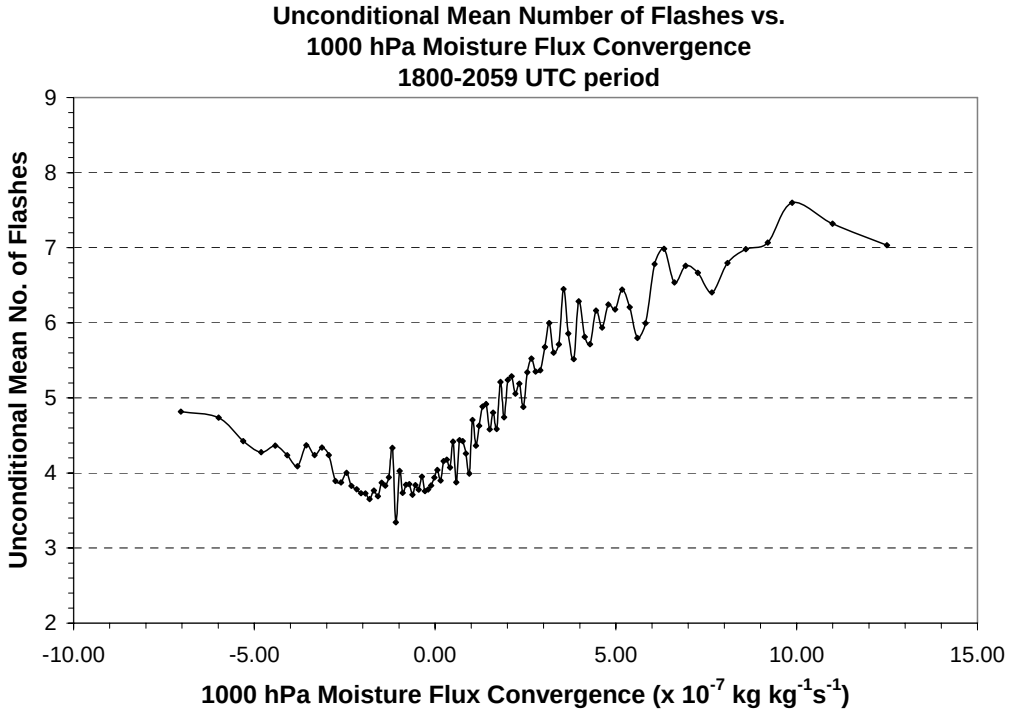

FIG. 8. Plots for a) the frequency of one or more flashes, and b) the unconditional mean number of flashes as a function of 1000 hPa moisture flux convergence for all regions combined during the 1800-2059 UTC period.

a)

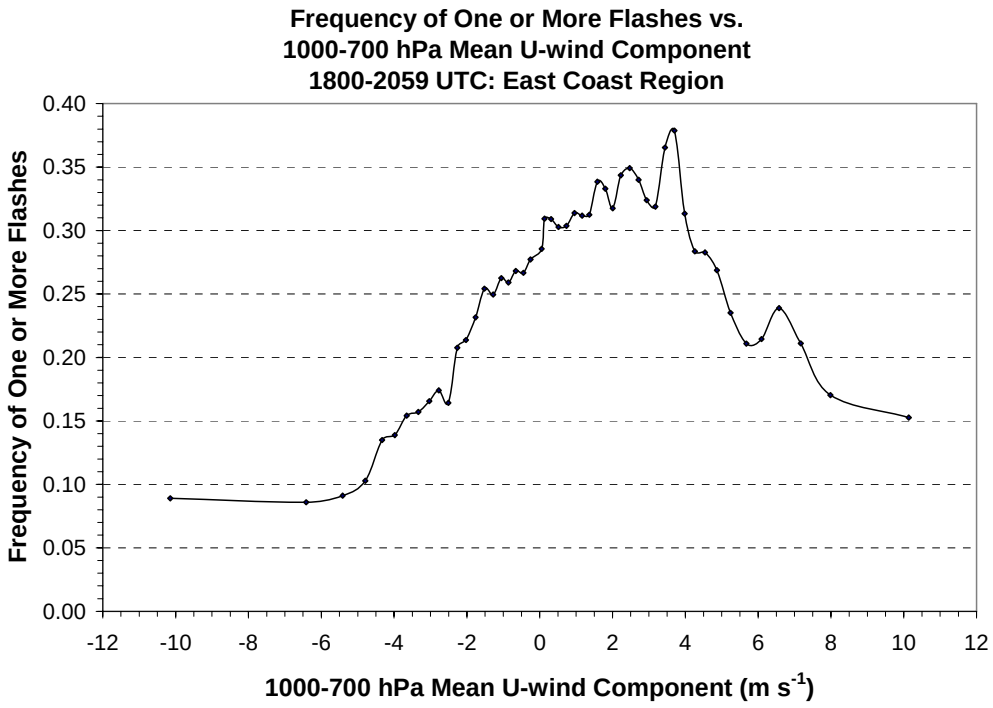

b)

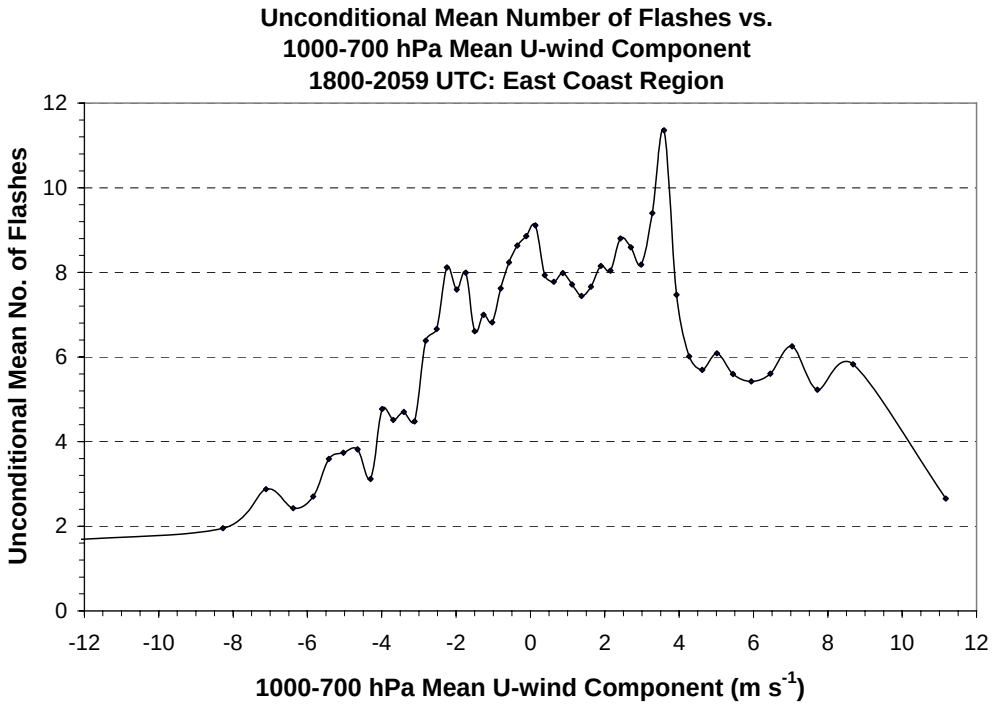

FIG. 9. Plots for a) the frequency of one or more flashes, and b) the unconditional mean number of flashes, as a function of 1000-700 hPa mean u-wind component for the East Coast region (1800-2059 UTC period).

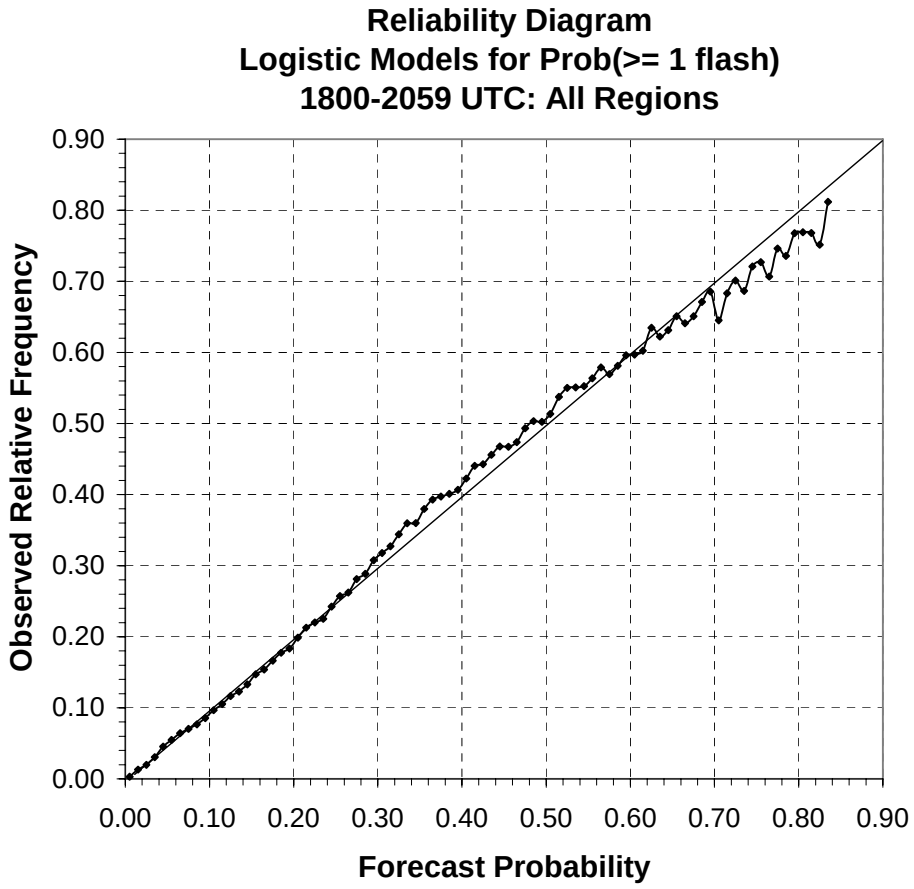

FIG. 10. Reliability diagram for the logistic models predicting the probability of one or more flashes. The results are for the dependent data sample and all regions combined during the 1800-2059 UTC period.

a)

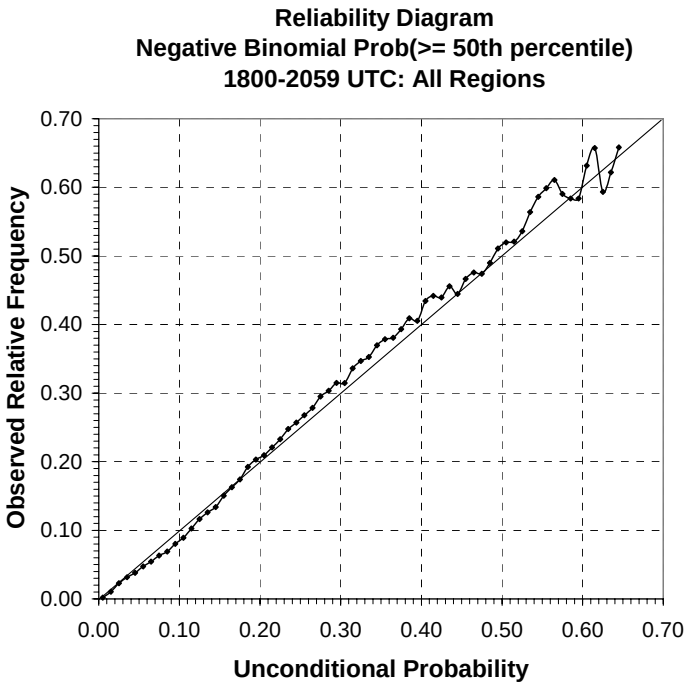

b)

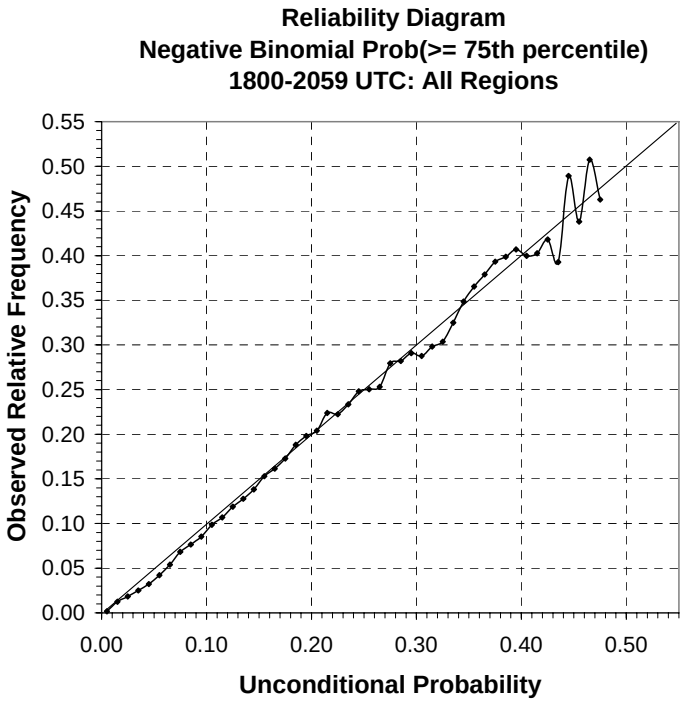

FIG. 11. Reliability diagrams for the unconditional probability of a) $\geq 50^{th}$, b) $\geq 75^{th}$, c) $\geq 90^{th}$, and d) $\geq 95^{th}$ percentiles of flash count. The results are for the dependent data sample and all regions combined during the 1800-2059 UTC period.

c)

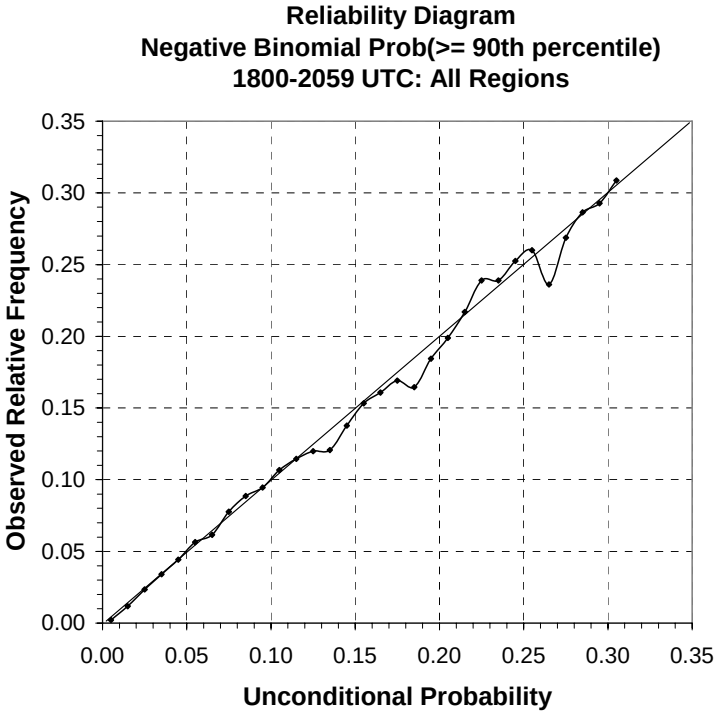

d)

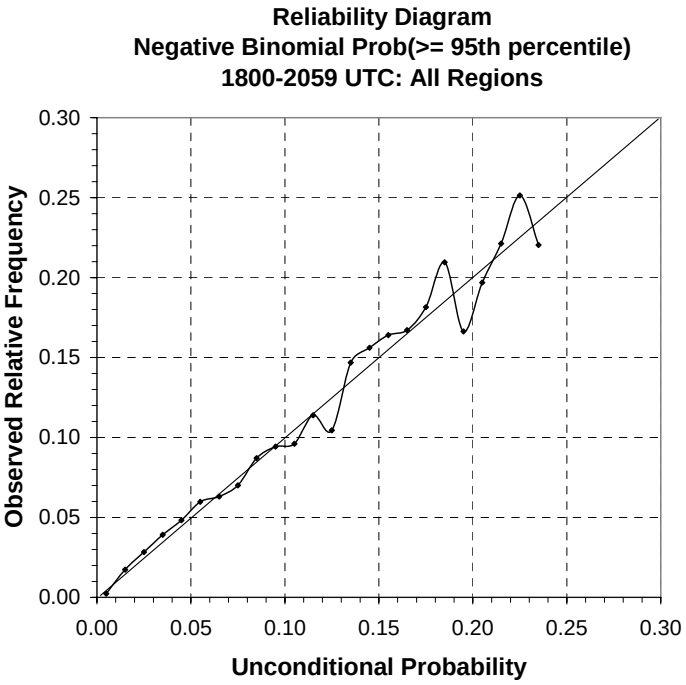

FIG. 11 (continued).

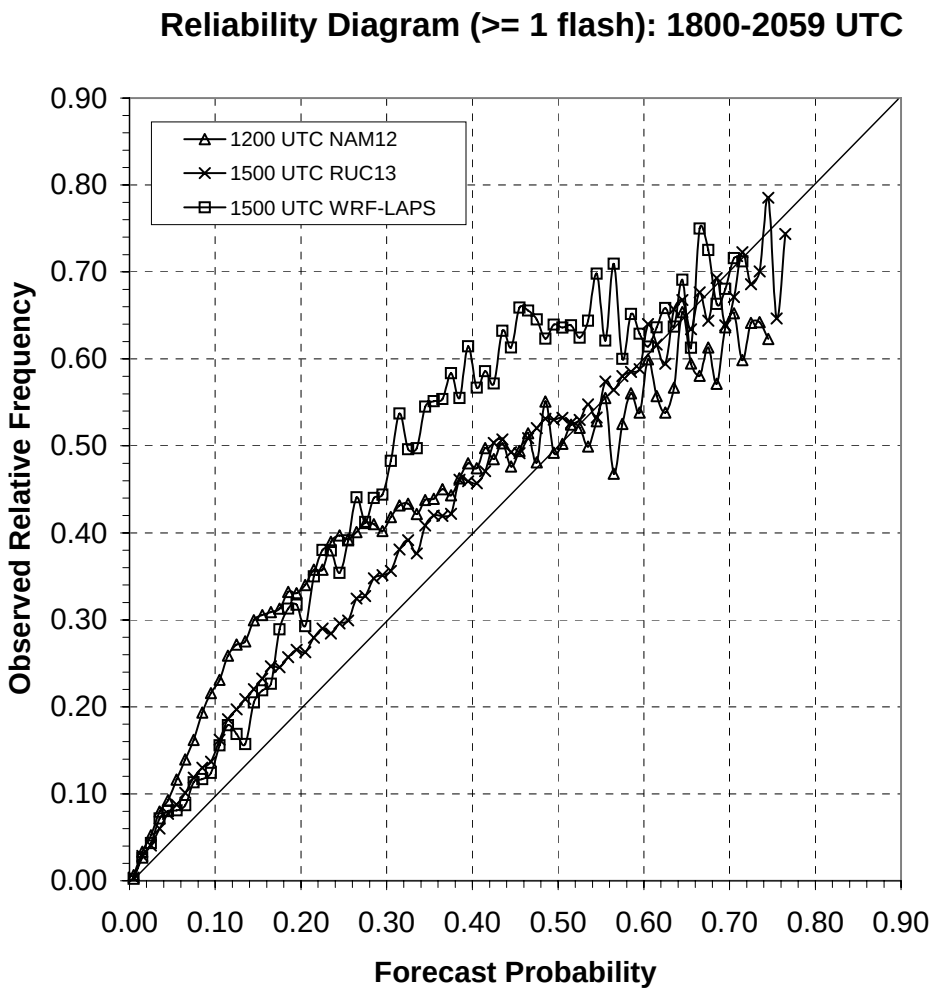

FIG. 12. Reliability diagram for the logistic models predicting the probability of one or more flashes during the 2006 independent test period. Results for the 1200 UTC NCEP NAM12, the 1500 UTC NCEP RUC13, and the 1500 UTC 4-km WRF-LAPS are shown for the 1800-2059 UTC period.

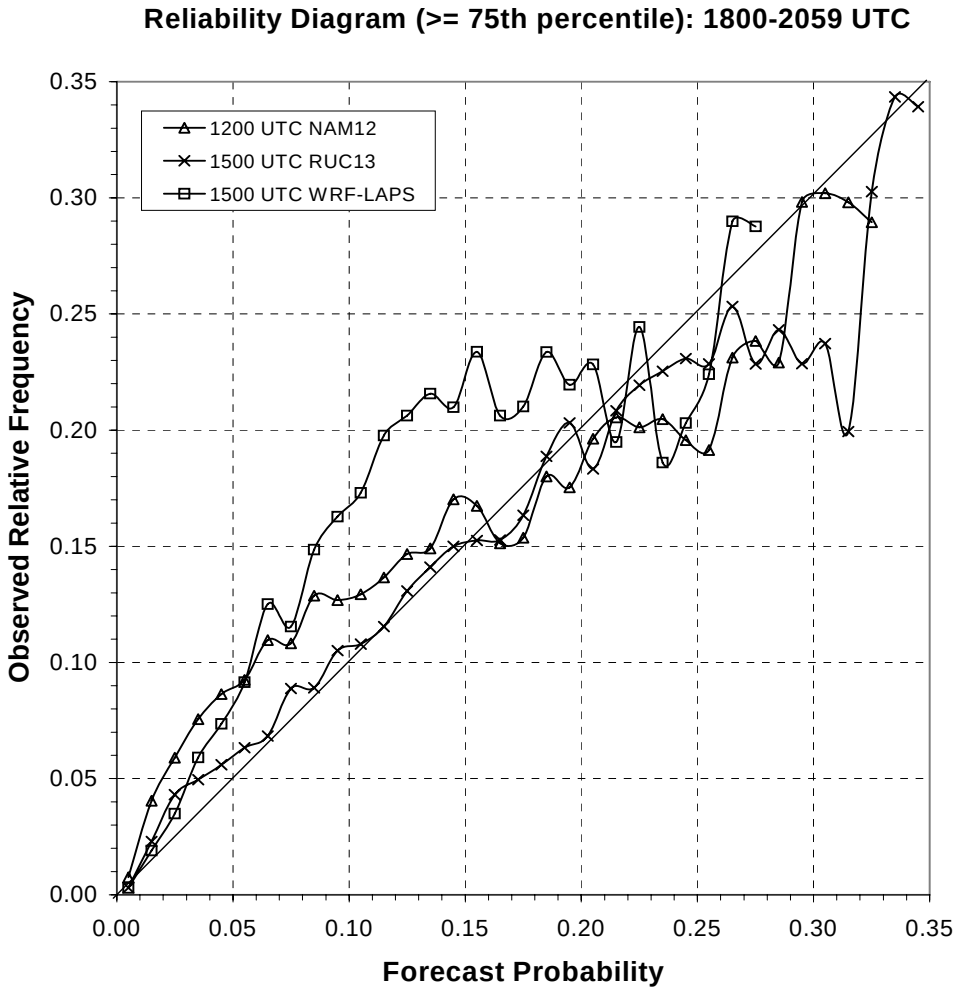

FIG. 13. Reliability diagram for the negative binomial models predicting the probability of $\geq 75^{th}$ percentile of flash count during the 2006 independent test period. Results for the 1200 UTC NCEP NAM12, the 1500 UTC NCEP RUC13, and the 1500 UTC 4-km WRF-LAPS are shown for the 1800-2059 UTC period.

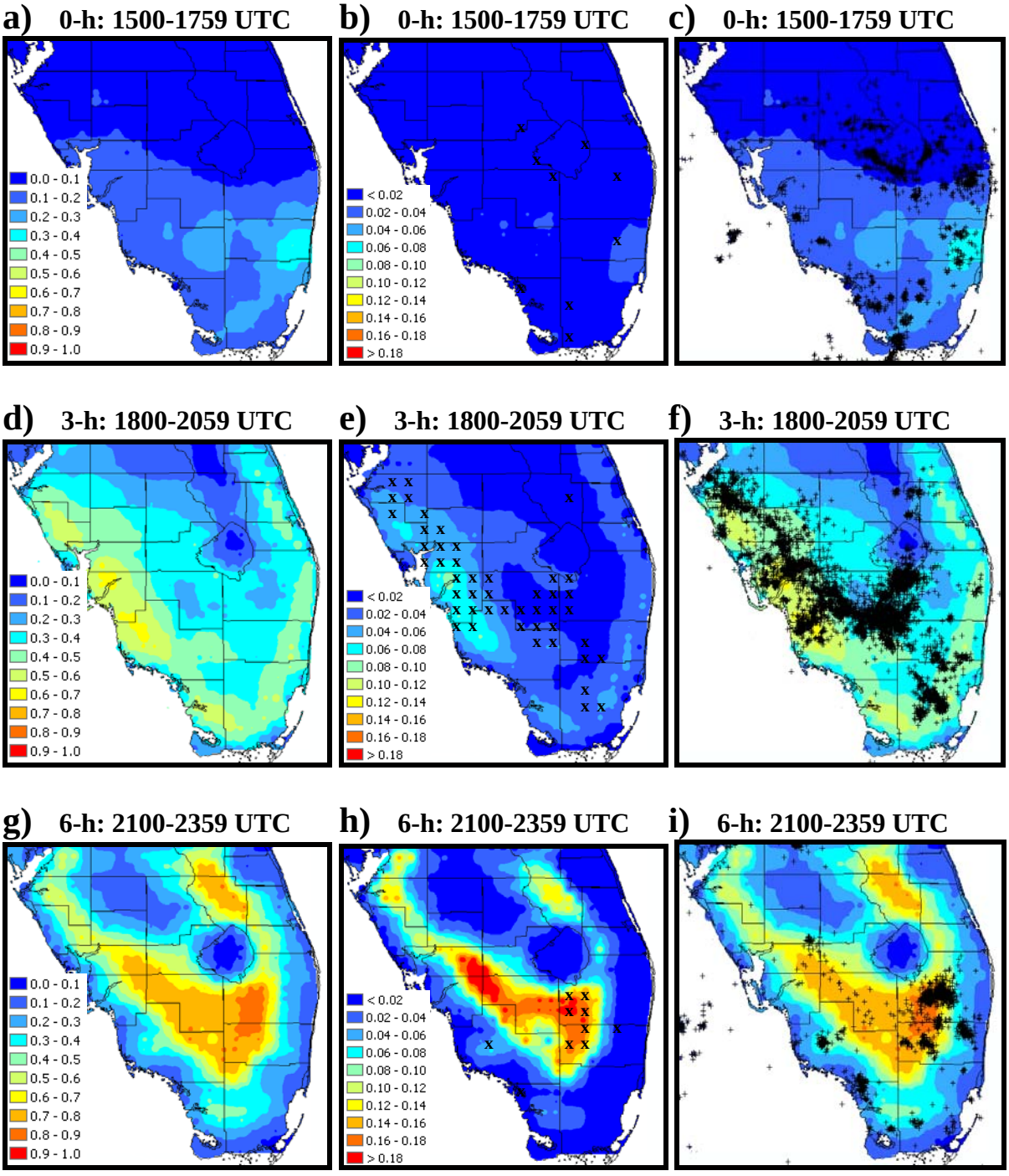

FIG. 14. Probability of one or more flashes (left panels), unconditional probability of ≥ 90th percentile (center panels), and CG strike verification superimposed on the one or more flash probabilities (right panels) for 16-17 August 2006 based on 1500 UTC WRF-LAPS (a-c) 0-h, (d-f) 3-h, (g-i) 6-h, and (j-l) 9-h forecast projections. Valid time periods are shown above each plot. Note the different color scales for the left and center panels. Grid points that received ≥ 90th percentile of flash count are indicated by the "x" symbols on the center panels.

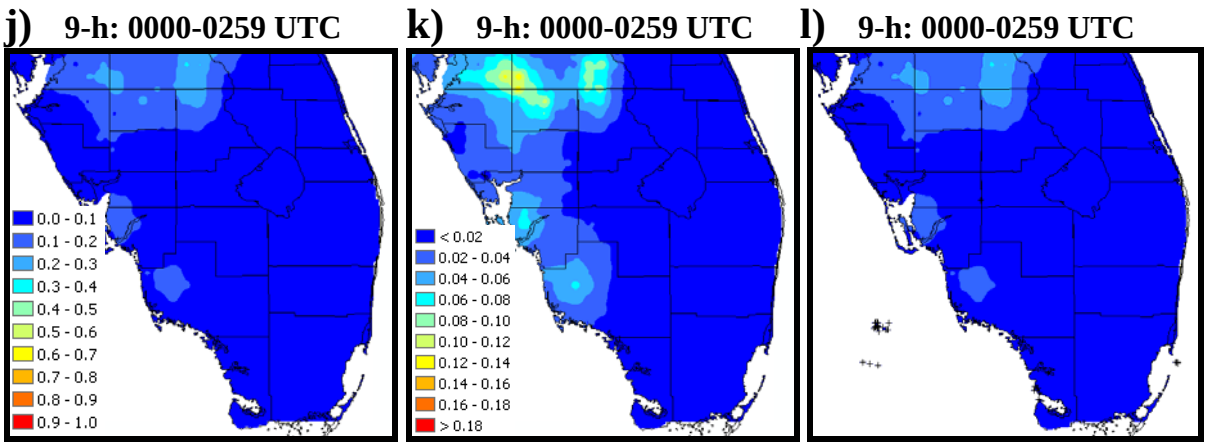

FIG. 14 (continued).

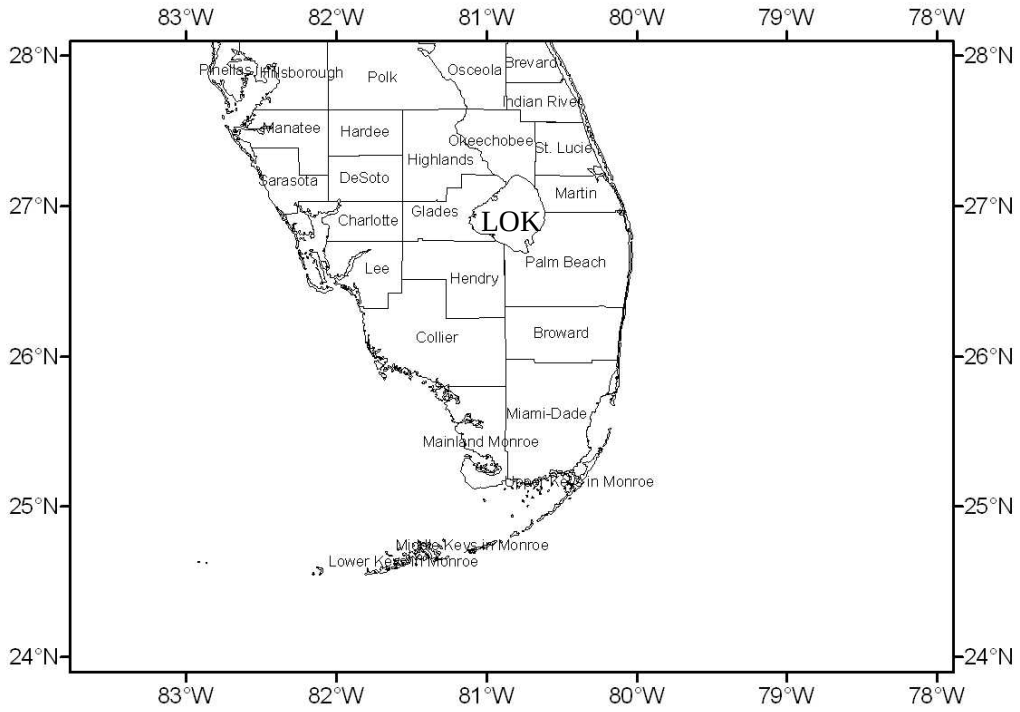

FIG. 15. Map of South Florida with county names and geographical features labeled.

TABLE 1. Conditional percentiles of CG flash count for the four most active 3-h periods. The percentiles are based on CG flash counts for all land grid points in the domain during eleven warm season periods (1995-2005).

	Percentile				
Time period (UTC)	50th	75th	90th	95th	Max
1500 – 1759	4	14	37	60	810
1800 – 2059	6	22	62	104	1190
2100 – 2359	5	21	65	114	1577
0000 – 0259	4	14	45	83	1267

TABLE 2. Number of RUC-analyzed sea-level pressure maps classified into each type at a correlation threshold of 0.70, using 3-houly data from the 1998-2005 warm seasons (9613 available maps). For purposes of developing the equations, maps which could not be classified into a type were assigned the type with which they were most correlated.

Map Type	No. Maps	% of Sample
A	2913	30.3
B	1303	13.6
C	1260	13.1
D	1061	11.0
E	1002	10.4
Unclassified	2074	21.6
Total	9613	100

TABLE 3. RUC-analyzed parameters investigated for inclusion in the candidate predictor pool. The name of each variable, a description (where needed), and abbreviations are included.

Abbrev.	Name	Description/levels
LTHICK	Layer thickness	1000-850 hPa, 850-500 hPa, 700-400 hPa, 500-300 hPa
TADV	Temperature advection	10 m and each 25 hPa surface
TCONV	Convective temperature	
CCTHICK	Cold cloud thickness	Thickness between 0°C level and cloud top (equil. level)
MFLXC	Moisture flux convergence	10 m and each 25 hPa surface
THEADV	Theta-e advection	10 m and each 25 hPa surface
PRECPW	Precipitable water	Entire depth of sounding (surface-100 hPa)
LAYRH	Layer mean relative humidity	45 layers between 1000 hPa and 100 hPa
RHFRZL	Relative humidity at 0°C level	
WBZP	Wet bulb zero pressure	
LCLP	Pressure at LCL	Lifting condensation level
MUCAPE	Most unstable CAPE	Largest CAPE obtained when each parcel between the surface and 700 hPa is lifted.
LCAPE1	MUCAPE in various layers	Cloud base to cloud top (Solomon and Baker 1994)
LCAPE2		Cloud base to –20°C (Bothwell 2002)
LCAPE3		Mixed phase region: 0°C to –40°C (Randell et al. 1994)
LCAPE4		Charging zone: -10°C to –25°C (Solomon and Baker 1994)
LCAPE5		Between –15°C and –20°C (Bothwell 2002)
NCAPE(1-5)	Normalized LCAPE	Layer CAPE divided by the geometric thickness of the layer
CIN	Convective inhibition	Negative area between the surface and 700 hPa by lifting the surface parcel.
BESTLI	Best Lifted Index (LI)	Most unstable LI obtained when each parcel between the surface and 700 hPa is lifted.
SSI	Showalter Stability Index	Lifted index based on parcel originating at 850 hPa
TT	Total Totals Index	as defined in the AMS Glossary of Meteorology (2000)
KI	K-index	as defined in the AMS Glossary of Meteorology (2000)
SWEAT	Severe Weather Threat Index	as defined in the AMS Glossary of Meteorology (2000)
TLAPSE	Temperature lapse rate	300-hPa layers between 1000 hPa and 100 hPa
THELAPSE	Theta-e lapse rate	300-hPa layers between 1000 hPa and 100 hPa
CCTHGT	Convective cloud top height	Geometric height of equilibrium level
PRFREQ	Price & Rind frequency	Price & Rind function for lightning frequency based on cloud top height: $F = (3.44 \times 10^{-5}) \times CCTHGT^{4.9}$
DIV	Wind divergence	10 m and each 25 hPa surface
VORT	Vorticity	10 m and each 25 hPa surface
VORTADV	Vorticity advection	10 m and each 25 hPa surface
MEANU	Layer average u component	45 layers between 1000 hPa and 100 hPa
MEANV	Layer average v component	45 layers between 1000 hPa and 100 hPa
MEANSP	Layer average speed	45 layers between 1000 hPa and 100 hPa
SHEAR	Layer wind shear	45 layers between 1000 hPa and 100 hPa

TABLE 4. Final list of RUC-derived candidate predictors used to develop the regression models. Power terms and two-way cross products for each parameter also were included in the final predictor pool (not listed). Spearman rank correlations with the binary (yes/no) lightning predictands for the 1800-2059 UTC period also are shown for the East Coast region.

Abbreviation	Name/description	Correlation
PRECPW	Precipitable water	0.36
KI	K-index	0.33
SSI	Showalter Stability Index	-0.30
LCAPE2	MUCAPE cloud base to -20°C	0.29
BESTLI	Best Lifted Index (LI)	-0.28
LCAPE4	MUCAPE -10°C to -25°C	0.26
CCTHICK	Cold cloud thickness	0.25
LCAPE5	MUCAPE -15°C to -20°C	0.24
TT	Total Totals Index	0.24
LTHICK1	1000-850 hPa thickness	0.23
TLAPSE2	900-600 hPa temperature lapse rate	-0.23
THELAPSE6	500-200 hPa theta-e lapse rate	-0.20
MFLXC2	1000 hPa Moisture flux convergence	0.20
LCLP	Pressure at LCL	0.19
DIV2	1000 hPa wind divergence	-0.17
TADV4	950 hPa temperature advection	0.14
MEANSP3	1000-700 hPa wind speed	-0.13
MEANV3	1000-700 hPa v component	0.13
DIV34	200 hPa wind divergence	0.11
THEADV5	925 hPa Theta-e advection	0.11
VORT2	1000 hPa vorticity	0.10
MEANU3	1000-700 hPa u component	0.10
LTHICK4	700-400 hPa thickness	0.09
CIN	Convective inhibition	0.08

TABLE 5. Logistic regression models for the probability of one or more flashes during the 1800-2059 UTC period. The regression coefficients for each of the four regions are shown. Parameters not selected for inclusion are indicated by -----.

Predictor	**East Coast**	**West Coast**	**Panhandle**	**AL & GA**
PRECPW	1.628	1.461	1.396	1.326
$(PRECPW)^2$	-0.400	-0.387	-0.474	-0.491
BESTLI	-0.357	-0.641	-0.633	-0.563
MFLXC2	0.312	0.218	0.321	0.385
MTFREQ	0.296	0.242	0.400	0.216
THEADV5	-----	0.132	0.103	-----
TLAPSE2	-0.546	-----	-----	-----
DIV34	-----	-----	0.152	0.133
(MEANU3) x (DISTEC)	-0.385	-----	-----	-----
$(MEANU3)^2$ x (DISTEC)	0.131	-----	-----	-----
(MEANU3) x (DISTWC)	-----	0.116	-----	-----
MEANU3	-----	-----	-----	0.237
MEANV3	-----	-----	-0.093	0.097
MEANSP3	-0.228	-0.418	-----	-----
SINDAY	0.100	0.181	0.066	0.123
Constant	-2.160	-1.881	-1.898	-1.940

TABLE 6. Negative Binomial regression models for the number of flashes during the 1800-2059 UTC period. The regression coefficients and the estimated shape parameter for each of the four regions are shown. Parameters not selected for inclusion are indicated by -----.

Predictor	**East Coast**	**West Coast**	**Panhandle**	**AL & GA**
MTMEAN	0.156	0.165	0.325	0.414
BESTLI	-0.188	-0.238	-0.252	-0.216
KI	0.126	0.153	0.106	-----
MFLXC2	0.139	0.069	0.107	-----
TLAPSE2	-0.235	-----	-----	-0.156
THELAPSE6	-----	-----	-----	-0.102
THEADV5	0.112	0.083	-----	-----
DIV2	-----	-----	-----	-0.158
DIV34	-----	-----	0.122	-----
MEANU3	0.147	-----	-----	0.056
$(MEANU3)^2$	-0.099	-----	-----	-----
MEANV3	-----	-----	-0.247	-0.174
MEANSP3	-----	-0.280	-----	-----
SINDAY	0.114	0.055	-----	-----
Constant	3.083	2.992	3.028	3.113
Shape parameter (θ)	0.369	0.373	0.368	0.377

TABLE 7. Verification scores for the 2006 independent test period for forecasting the probability of one or more CG flashes. Brier Scores for the model, L-CLIPER, and persistence alone are shown for the 1200 UTC NCEP NAM12 (top), the 1500 UTC NCEP RUC13 (middle), and the 1500 UTC WRF-LAPS (bottom). The rightmost column shows the percent improvement in Brier Score with respect to L-CLIPER (left) and persistence alone (right).

1200 UTC NCEP NAM12
21 June – 30 September, 2006 (all grid points)

Forecast Projection	Forecast Valid Period (UTC)	Brier Score Model	Brier Score L-CLIPER	Brier Score Persistence	Brier Skill Scores (%)
3-h	1500-1759	0.075	0.079	0.081	4.5 / 6.5
6-h	1800-2059	0.159	0.164	0.171	2.5 / 6.8
9-h	2100-2359	0.163	0.160	0.167	-1.8 / 2.0
12-h	0000-0259	0.087	0.078	0.079	-12.0 / -10.8
15-h	0300-0559	0.023	0.022	0.022	-6.7 / -6.4

1500 UTC NCEP RUC13
1 May – 30 September, 2006 (all grid points)

Forecast Projection	Forecast Valid Period (UTC)	Brier Score Model	Brier Score L-CLIPER	Brier Score Persistence	Brier Skill Scores (%)
0-h	1500-1759	0.062	0.070	0.072	11.7 / 14.1
3-h	1800-2059	0.128	0.143	0.152	10.8 / 16.0
6-h	2100-2359	0.129	0.138	0.144	6.8 / 10.9
9-h	0000-0259	0.071	0.069	0.070	-2.8 / -2.1
12-h	0300-0559	0.025	0.025	0.025	0.2 / -0.1

1500 UTC WRF-LAPS
1 August – 30 September, 2006 (South Florida domain)

Forecast Projection	Forecast Valid Period (UTC)	Brier Score Model	Brier Score L-CLIPER	Brier Score Persistence	Brier Skill Scores (%)
0-h	1500-1759	0.125	0.128	0.132	2.0 / 5.1
3-h	1800-2059	0.197	0.212	0.226	7.2 / 13.0
6-h	2100-2359	0.194	0.193	0.202	-0.5 / 3.7
9-h	0000-0259	0.087	0.077	0.077	-13.7 / -14.1
12-h	0300-0559	0.014	0.013	0.013	-3.2 / -3.4

TABLE 8. Verification scores for the 2006 independent test period for forecasting the probability of ≥ 75th percentile of flash count. Brier Scores for the model, L-CLIPER, and persistence alone are shown for the 1200 UTC NCEP NAM12 (top), the 1500 UTC NCEP RUC13 (middle), and the 1500 UTC WRF-LAPS (bottom). The rightmost column shows the percent improvement in Brier Score with respect to L-CLIPER (left) and persistence alone (right).

1200 UTC NCEP NAM12
21 June – 30 September 2006 (all grid points)

Forecast Projection	Forecast Valid Period (UTC)	Brier Score Model	Brier Score L-CLIPER	Brier Score Persistence	Brier Skill Scores (%)
3-h	1500-1759	0.185	0.187	0.188	1.3 / 1.4
6-h	1800-2059	0.185	0.190	0.190	2.5 / 2.6
9-h	2100-2359	0.195	0.194	0.193	-0.4 / -0.6
12-h	0000-0259	0.195	0.192	0.192	-1.8 / -1.7

1500 UTC NCEP RUC13
1 May – 30 September 2006 (all grid points)

Forecast Projection	Forecast Valid Period (UTC)	Brier Score Model	Brier Score L-CLIPER	Brier Score Persistence	Brier Skill Scores (%)
0-h	1500-1759	0.188	0.191	0.191	1.4 / 1.7
3-h	1800-2059	0.186	0.192	0.192	3.1 / 3.1
6-h	2100-2359	0.187	0.194	0.193	3.8 / 3.5
9-h	0000-0259	0.203	0.195	0.195	-4.2 / -4.2

1500 UTC WRF-LAPS
1 August – 30 September 2006 (South Florida domain)

Forecast Projection	Forecast Valid Period (UTC)	Brier Score Model	Brier Score L-CLIPER	Brier Score Persistence	Brier Skill Scores (%)
0-h	1500-1759	0.177	0.181	0.184	2.2 / 3.4
3-h	1800-2059	0.186	0.195	0.195	4.3 / 4.5
6-h	2100-2359	0.183	0.188	0.188	2.7 / 2.6
9-h	0000-0259	0.206	0.196	0.198	-5.1 / -4.1

TABLE 9. Verification scores for the 2006 independent test period for forecasting the probability of one or more CG flashes. This is the same as Table 8, except using relaxed verification criteria. In this case the forecast probability is the maximum probability within a 20-km radius of each grid point.

1200 UTC NCEP NAM12
21 June – 30 September, 2006 (all grid points)

Forecast Projection	Forecast Valid Period (UTC)	Brier Score Model	Brier Score L-CLIPER	Brier Score Persistence	Brier Skill Scores (%)
3-h	1500-1759	0.073	0.080	0.080	8.7 / 9.0
6-h	1800-2059	0.153	0.165	0.169	7.1 / 9.1
9-h	2100-2359	0.169	0.160	0.164	-6.1 / -3.8
12-h	0000-0259	0.096	0.078	0.078	-23.8 / -22.9
15-h	0300-0559	0.025	0.022	0.022	-14.8 / -14.7

1500 UTC NCEP RUC13
1 May – 30 September, 2006 (all grid points)

Forecast Projection	Forecast Valid Period (UTC)	Brier Score Model	Brier Score L-CLIPER	Brier Score Persistence	Brier Skill Scores (%)
0-h	1500-1759	0.061	0.070	0.071	13.1 / 14.6
3-h	1800-2059	0.125	0.144	0.151	12.6 / 16.6
6-h	2100-2359	0.127	0.137	0.142	7.3 / 10.5
9-h	0000-0259	0.071	0.069	0.069	-3.8 / -3.4
12-h	0300-0559	0.025	0.025	0.025	0.1 / 0.1

1500 UTC WRF-LAPS
1 August – 30 September, 2006 (South Florida domain)

Forecast Projection	Forecast Valid Period (UTC)	Brier Score Model	Brier Score L-CLIPER	Brier Score Persistence	Brier Skill Scores (%)
0-h	1500-1759	0.121	0.128	0.130	5.3 / 6.6
3-h	1800-2059	0.184	0.211	0.219	12.7 / 16.0
6-h	2100-2359	0.212	0.194	0.198	-9.3 / -6.9
9-h	0000-0259	0.099	0.072	0.077	-28.4 / -29.5
12-h	0300-0559	0.014	0.014	0.014	-0.5 / -0.4

TABLE 10. Verification scores for the 2006 independent test period for forecasting the probability of $\geq 75^{th}$ percentile of flash count. This is the same as Table 9, except using relaxed verification criteria. In this case the forecast probability is the maximum probability within a 20-km radius of each grid point.

1200 UTC NCEP NAM12
21 June – 30 September 2006 (all grid points)

Forecast Projection	Forecast Valid Period (UTC)	Brier Score Model	Brier Score L-CLIPER	Brier Score Persistence	Brier Skill Scores (%)
3-h	1500-1759	0.184	0.190	0.188	3.1 / 2.2
6-h	1800-2059	0.185	0.192	0.191	3.9 / 3.0
9-h	2100-2359	0.201	0.196	0.194	-2.4 / -3.3
12-h	0000-0259	0.198	0.193	0.192	-2.4 / -2.8

1500 UTC NCEP RUC13
1 May – 30 September 2006 (all grid points)

Forecast Projection	Forecast Valid Period (UTC)	Brier Score Model	Brier Score L-CLIPER	Brier Score Persistence	Brier Skill Scores (%)
0-h	1500-1759	0.189	0.192	0.191	1.7 / 1.1
3-h	1800-2059	0.188	0.194	0.192	3.3 / 2.5
6-h	2100-2359	0.188	0.196	0.195	4.1 / 3.2
9-h	0000-0259	0.202	0.195	0.195	-3.1 / -3.4

1500 UTC WRF-LAPS
1 August – 30 September 2006 (South Florida domain)

Forecast Projection	Forecast Valid Period (UTC)	Brier Score Model	Brier Score L-CLIPER	Brier Score Persistence	Brier Skill Scores (%)
0-h	1500-1759	0.177	0.184	0.184	3.6 / 3.7
3-h	1800-2059	0.186	0.199	0.197	6.4 / 5.3
6-h	2100-2359	0.192	0.193	0.192	0.3 / 0.2
9-h	0000-0259	0.199	0.189	0.190	-5.3 / -4.7